

Accepted Manuscript

Design and synthesis of novel xanthone-triazole derivatives as potential antidiabetic agents: α -Glucosidase inhibition and glucose uptake promotion

Gao-Jie Ye, Tian Lan, Zhi-Xin Huang, Xiao-Ning Cheng, Chao-Yun Cai, Sen-Miao Ding, Min-Li Xie, Bo Wang



PII: S0223-5234(19)30455-6

DOI: <https://doi.org/10.1016/j.ejmech.2019.05.045>

Reference: EJMECH 11355

To appear in: *European Journal of Medicinal Chemistry*

Received Date: 18 February 2019

Revised Date: 15 May 2019

Accepted Date: 16 May 2019

Please cite this article as: G.-J. Ye, T. Lan, Z.-X. Huang, X.-N. Cheng, C.-Y. Cai, S.-M. Ding, M.-L. Xie, B. Wang, Design and synthesis of novel xanthone-triazole derivatives as potential antidiabetic agents: α -Glucosidase inhibition and glucose uptake promotion, *European Journal of Medicinal Chemistry* (2019), doi: <https://doi.org/10.1016/j.ejmech.2019.05.045>.

This is a PDF file of an unedited manuscript that has been accepted for publication. As a service to our customers we are providing this early version of the manuscript. The manuscript will undergo copyediting, typesetting, and review of the resulting proof before it is published in its final form. Please note that during the production process errors may be discovered which could affect the content, and all legal disclaimers that apply to the journal pertain.

Design and synthesis of novel xanthone-triazole derivatives as potential antidiabetic agents: α -glucosidase inhibition and glucose uptake promotion

Gao-Jie Ye ^a, Tian Lan ^a, Zhi-Xin Huang ^a, Xiao-Ning Cheng ^b, Chao-Yun Cai ^c, Sen-Miao Ding ^a, Min-Li Xie ^a, Bo Wang ^{a*}

^a School of Chemistry, Sun Yat-sen University, 135 Xingang West Road, Guangzhou, 510275, PR China

^b Instrumental Analysis & Research Center, Sun Yat-sen University, 135 Xingang West Road, Guangzhou, 510275, PR China

^c Department of Pharmaceutical Sciences, College of Pharmacy and Health Sciences, St. John's University, 8000 Utopia Parkway, Queens, New York 11439, United States

Keywords: xanthone-triazole derivatives, α -glucosidase inhibitors, noncompetitive, molecular docking, cytotoxicity, glucose uptake

Abstract:

Inhibiting the decomposition of carbohydrates into glucose or promoting glucose conversion is considered to be an effective treatment for type 2 diabetes. Herein, a series of novel xanthone-triazole derivatives were designed, synthesized, and their α -glucosidase inhibitory activities and glucose uptake in HepG2 cells were investigated. Most of the compounds showed better inhibitory activities than the parental compound **a** (1,3-dihydroxyxanthone, $IC_{50} = 160.8 \mu M$) and 1-deoxynojirimycin (positive control, $IC_{50} = 59.5 \mu M$) towards α -glucosidase. Compound **5e** was the most potent inhibitor, with IC_{50} value of $2.06 \mu M$. The kinetics of enzyme inhibition showed that compounds **5e**, **5g**, **5h**, **6c**, **6d**, **6g** and **6h** were noncompetitive inhibitors, and molecular docking results were consistent with the noncompetitive property that these compounds bind to allosteric sites away from the active site (Asp214, Glu276 and Asp349). On the other hand, the glucose uptake assays exhibited that compounds **5e**, **6a**, **6c** and **7g** displayed high activities in

promoting the glucose uptake. The cytotoxicity assays showed that most compounds were low-toxic to human normal hepatocyte cell line (LO2). These novel xanthone triazole derivatives exhibited dual therapeutic effects of α -glucosidase inhibition and glucose uptake promotion, thus they could be use as antidiabetic agents for developing novel drugs against type 2 diabetes.

1. Introduction

Diabetes mellitus is a metabolic disorder characterized by prolonged hyperglycemia, which leads to an increased risk of cancer, stroke, cardiovascular disease, retinopathy, nephropathy, and metabolic syndrome [1-4]. According to the World Health Organization, more than 420 million people are suffering from diabetes, and the number would increase to 642 million in 2040 [5, 6]. Type 2 diabetes (Noninsulin-dependent diabetes mellitus) is the most common form of diabetes mellitus, accounting for more than 90 % of all diabetes cases [7].

The main strategy for treating this disease is to control the high blood glucose levels. The strategies to control blood glucose levels can be retarding, regulating and/or inhibiting carbohydrate hydrolytic enzymes [8]. α -Glucosidase (EC.3.2.1.20) is an important hydrolytic enzyme playing a vital role in digestion of carbohydrates and biosynthesis of viral envelope glycoproteins [9]. It catalyzes the final step of carbohydrates digestion in biological systems, and converts unabsorbed oligosaccharides and disaccharides into monosaccharides, thus resulting in hyperglycemia for diabetic patients [7, 10]. Hence, it is an effective therapeutic approach for type 2 diabetes by suppressing the activity of α -glucosidase. α -Glucosidase inhibitors can retard carbohydrates digestion through inhibiting the activity of α -glucosidase, which in turn balance postprandial blood glucose levels. The well-known α -glucosidase inhibitors, such as acarbose, miglitol and voglibose, have been used for the treatments of type 2 diabetes. However, it is attractive and meaningful to discover novel α -glucosidase inhibitors due to the adverse effects (for

instance, flatulence, diarrhoea, stomach ache and liver damage [11]) of the available α -glucosidase inhibitors.

The imbalances of glucose homeostasis in type 2 diabetes results in reduced glucose intake in peripheral tissues and increased hepatic glucose output [12]. The Liver plays a major role in blood glucose control and utilization, providing glucose to both insulin-sensitive (fat and skeletal muscle) and insulin-insensitive (nervous, skin, red blood cells, smooth muscle, etc.) tissues. Therefore, promoting glucose uptake in the liver is also an effective strategy for diabetic patients to control blood glucose levels [13].

Xanthone and their derivatives are widely distributed in nature and they exhibit various pharmacological activities, such as anti-inflammatory, anti-oxidant, anti-bacterial, anti-viral, anti-tumor etc. [14-16]. In the previous studies, we have shown that the synthetic polyhydroxyxanthenes, benzoxanthenes, noncoplanar xanthenes, 3-acyloxyxanthenes, and oxazolxanthenes, could be used as new classes of α -glycosidase inhibitors [17-21]. The IC_{50} values of the most compounds were ranging from 10-200 μ M. To further increase the activity, we hope to introduce appropriate groups at the suitable position of xanthone core. Therefore, we checked all the xanthone derivatives we synthesized, we noticed that introducing oxygen or nitrogen containing group and/or aromatic group into the C3 position of xanthone ring through the ether or ester bond would increase the inhibitory activities [17, 21] (Figure 1: (A)). Compound **b** as the ester derivatives of xanthone, is a representative compound, which exhibited much higher inhibitory activity than its parental compound **a** (Figure 1: (A)). Accordingly, we hypothesized that potential α -glycosidase inhibitors can be obtained by modifying the OH at the C3 position of xanthone ring, and this modification can be easily to achieve. Considering the ester-bearing compounds are thought to be susceptible to hydrolysis by intestinal esterases and the present groups (such as the groups of compounds **c**, **d** and **e**) introduced through the ether bond showed no so good inhibitory activities, thus,

introducing the other appropriate group at C3 position of xanthone through the ether bond could improve the stability and increase the inhibitory activity.

1,2,3-Triazole is a heterocyclic scaffold significantly widespread in the medicinal chemistry field. This scaffold is stable to acid/basic hydrolysis and reductive/oxidative conditions, showing high aromatic stabilization and resistance to metabolic degradation [22-24]. Previous studies showed that 1,2,3-triazole derivatives have a variety of biological activities, such as anti-cancer, anti-tuberculosis, anti-fungal, anti-bacterial, anti-HIV etc. [25]. Ferreira et al. synthesized a series of 4-substituted 1,2,3-triazoles. These compounds showed high α -glucosidase inhibitory activities and reduced the postprandial blood glucose levels in normal rats [23]. Wang et al. synthesized two series of 2,4,5-triarylimidazole-1,2,3-triazole derivatives and triazine-triazole derivatives. The biological activity test showed that all the triazole derivatives had good inhibitory activities towards α -glucosidase [26, 27].

At the same time, 1,2,3-triazole, with strong dipole moment, could actively participate in hydrogen bonding and π -stacking interactions [23]. In our previous research, π -stacking, hydrogen bonding and hydrophobic effect play key roles in promoting the α -glucosidase inhibitory activity [18, 19]. Considering the significant increase of inhibitory activities after the modification of xanthone at C3 position and the fact that 1,2,3-triazoles with potential metabolic stability and good α -glycosidase inhibitory activities, we designed the skeleton of xanthone-triazole (Figure 1: (B)). From prior docking studies, the skeleton compound exhibited a higher docking score (-9.02 kcal/mol) than compound **a** (-6.65 kcal/mol). It was also found that the nitrogen atom of the triazole and the oxygen atom of the amide bond formed hydrogen bonds with the enzyme (Figure 1: (C)), which may further enhance the binding of α -glucosidase and the compound, thus increasing the α -glucosidase inhibitory activity. The docking results rationalized the idea of introducing triazole into the parental compound **a**.

Thus, in this study, a novel series of xanthone derivatives substituted with triazole group at C3 position, and with OH, OMe or Br groups at C1, C6 or C7 position were synthesized (Scheme 1), and their *in vitro* α -glucosidase activities and inhibitory mechanism were evaluated. Moreover, molecular docking was performed to gain insight into possible binding modes with α -glucosidase.

Furthermore, it was reported that flavonoids could increase glucose uptake in HepG2 hepatocellular liver carcinoma cell line [28], and the xanthone-triazole derivatives have the common structure with these compounds (Figure 2), which enlightened us that the synthetic xanthone triazole derivatives may also promote glucose uptake in the live cells. Therefore, in order to determine whether the xanthone-triazole derivatives, which possessed high α -glucosidase inhibitory activities, can be used as potential anti-diabetes agents, glucose uptake and cytotoxicity assays were also carried out.

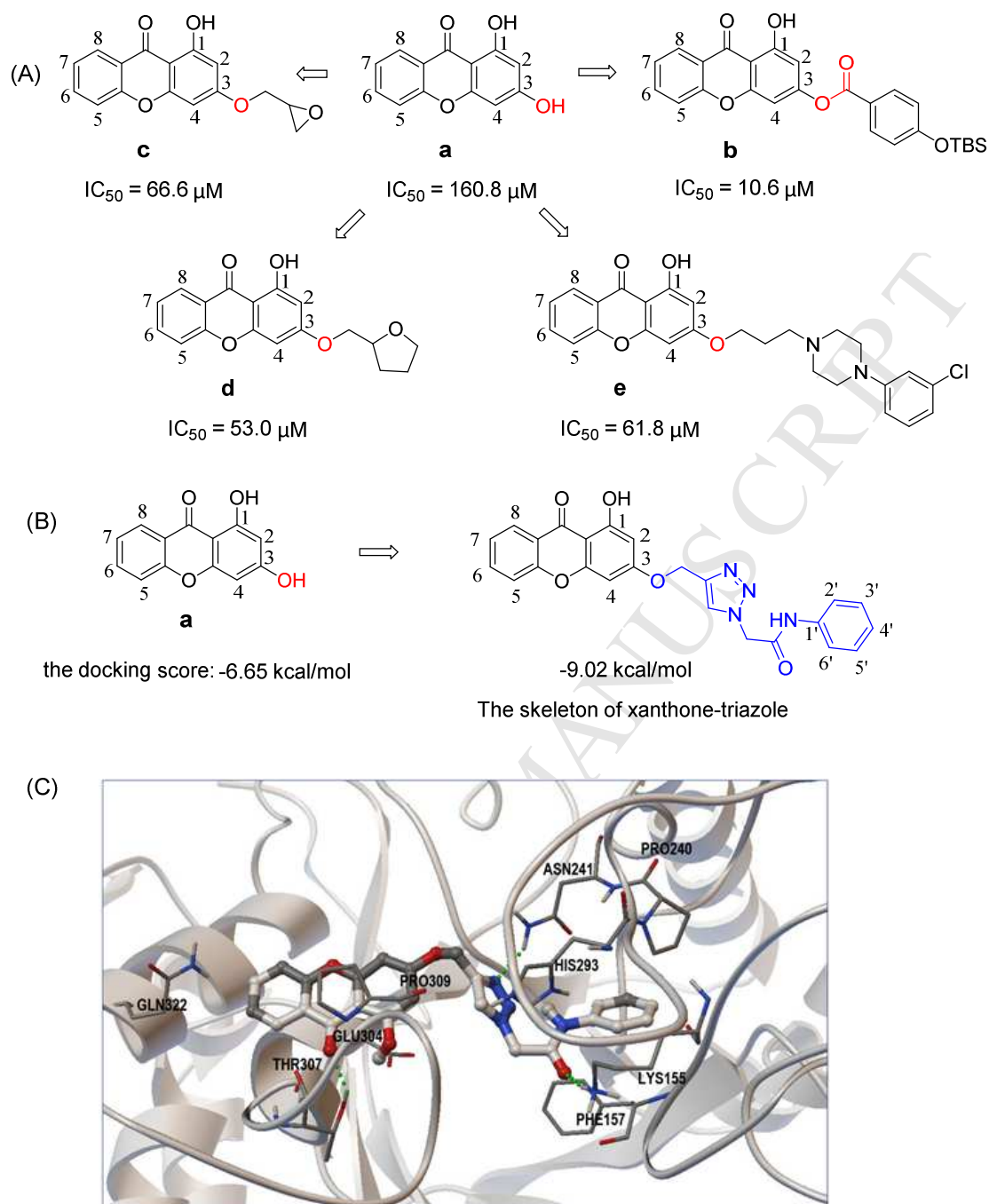


Figure 1. Xanthenes as α -glucosidase inhibitors and molecular docking of the xanthone-triazole's skeleton. (A) The synthetic xanthenes as the α -glucosidase inhibitors. (B) 1,3-dihydroxyxanthone and the skeleton of xanthone-triazole. (C) Predicted interactions of the skeleton of xanthone-triazole with α -glucosidase. The green dashed lines stand for hydrogen bonds.

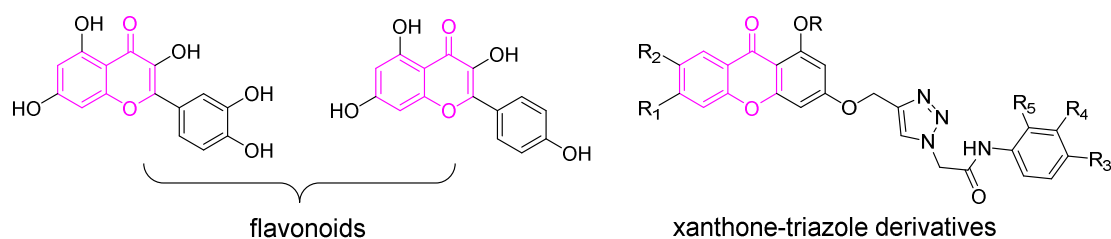
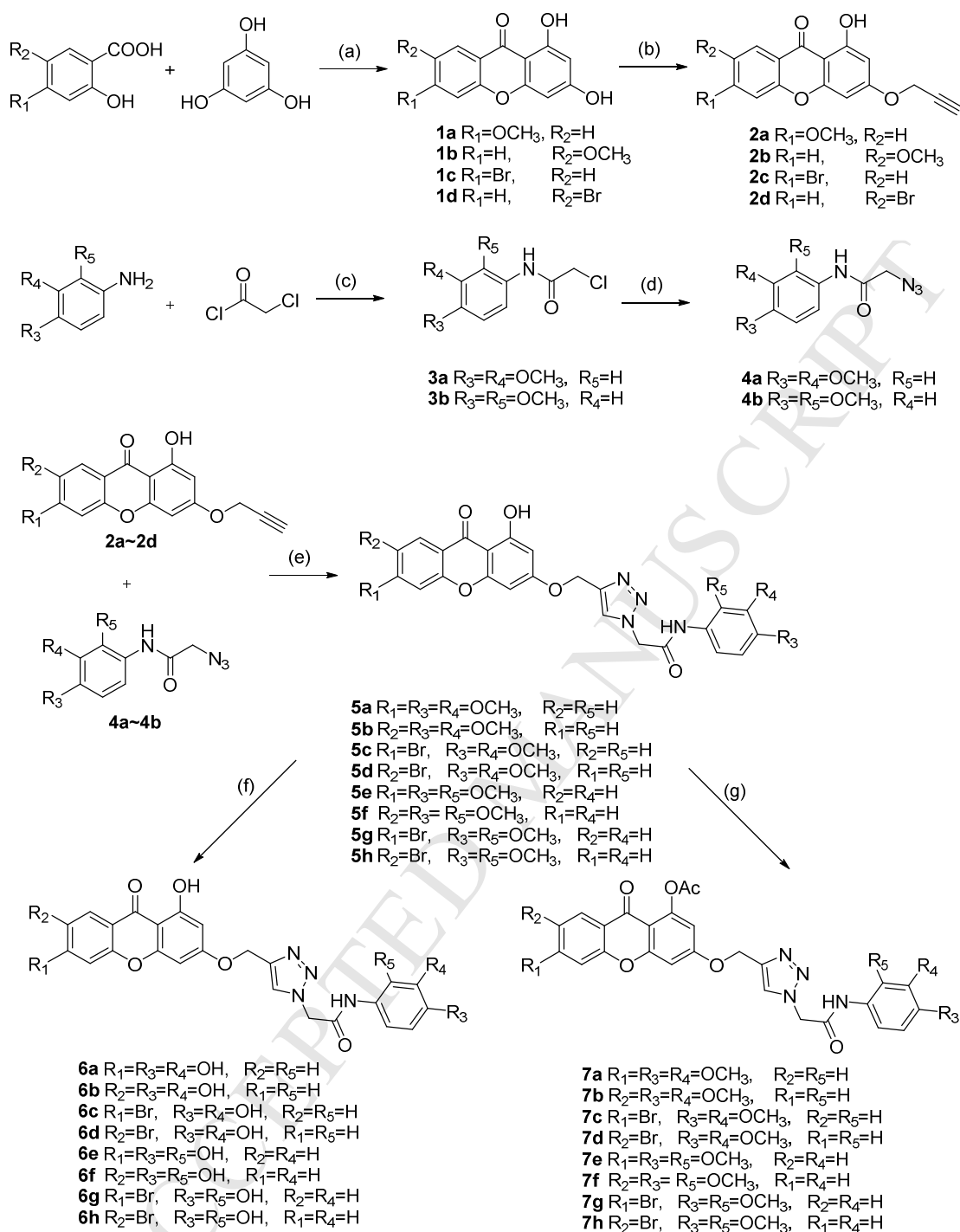


Figure 2. The structure of flavonoids and xanthone-triazole derivatives

2. Result and discussion

2.1 Chemistry

The xanthone-triazole derivatives **5a-5h**, **6a-6h**, **7a-7h** were synthesized as showed in Scheme 1. Compounds **1a-1d** were synthesized from different substituted hydroxybenzoic acids with phloroglucinol in the presence of Eaton's reagent [29]. Compounds **1a-1d** reacted with 3-bromopropyne in acetone at 60 °C for 5-14 h to produce **2a-2d** with the yields of 61-75% [30]. Different substituted anilines reacted with chloroacetyl chloride to obtain compounds **3a-3b** in 96 and 98 % yields, respectively [31]. Compounds **3a-3b** reacted with NaN₃ in DMF at room temperature for 4 h to generate the intermediates **4a-4b** [31, 32]. Then, intermediates **2a-2d** and **4a-4b** underwent copper(I)-catalyzed alkyne-azide cycloaddition (CuAAC) in the presence of CuSO₄·5H₂O and sodium ascorbate, then products **5a-5h** were obtained with the yields of 71-89 % [33]. Demethylation of compounds **5a-5h** in CH₂Cl₂ with a large excess BBr₃ gave products **6a-6h** in the yields of 22-45 % [34]. Finally, xanthone-triazole derivatives **7a-7h** were achieved with the yields of 81-93 % by the reaction of compounds **5a-5h** with Ac₂O under the catalysis of NaOAc at 90 °C [35].



Scheme 1. Synthesis of xanthone-triazole derivatives. Reagents and conditions: (a) Eaton's reagent, reflux; (b) 3-bromopropyne, K_2CO_3 , acetone, reflux; (c) dry THF, N_2 , 0 °C; (d) NaN_3 , DMF, 40 °C; (e) $CuSO_4 \cdot 5H_2O$, sodium ascorbate, DMF, rt; (f) BBr_3 , dry DCM, 0 °C; (g) Ac_2O , NaOAc, 90 °C.

2.2 α -Glucosidase inhibitory activities and structure-correlation analysis

The α -glucosidase inhibitory activities of all the synthetic compounds were assayed and the IC_{50} values were listed in Table 1.

As shown in the Table 1, all the synthetic compounds **5a-5h**, **6a-6h** and **7a-7h** showed higher inhibitory activities than the parental compound **a** and almost half of the compounds showed greater inhibition than compound **b** (Figure 1: (A)), which demonstrated that the introduction of triazole structure at the C3-OH position can increase the inhibitory activity as expected. More exciting results were that almost of the compounds showed higher inhibitory activities than 1-deoxynojirimycin (positive control) except **5b**, **7a** and **7b**, and the IC_{50} value of compound **5e** reached 2.06 μ M, nearly 29 folds lower than 1-deoxynojirimycin, and 78 folds lower than the parental compound **a**.

Compounds **7a-7h** showed lower inhibition compared with **5a-5h**, indicating that the inhibitory activities decreased when OH was changed to OAc at C1 position. These facts suggested that this OH was vital for the compound binding to the enzyme, probably involved in hydrogen bonding or other electrostatic interaction with the enzyme.

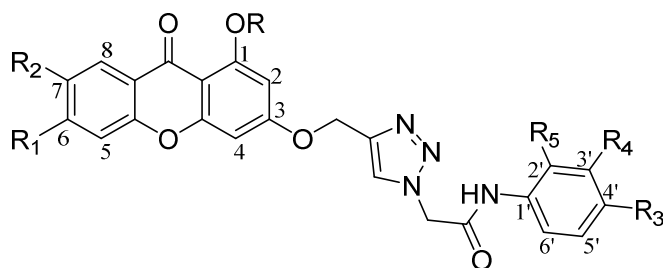
Comparing the IC_{50} values of the pair of compounds **a/c**, **b/d**, **e/g** and **f/h** among all the series, it was found that the inhibitory activity was enhanced when the OH or OCH_3 group at the C6 or C7 of xanthone ring were replaced by Br except **5g**. In our previous QASR studies, it revealed that the chemical softness of the groups was a key factor influencing the inhibitory activity [36]. Based on this, we hypothesized that the chemical softness of Br might be the key factors in promoting the inhibitory activity.

Comparing the IC_{50} values of compounds **5a-5h** bearing OCH_3 at different positions of the aromatic rings and **6a-6h** with OCH_3 reduced to OH, respectively. The results showed that **6a-6d** exhibited higher inhibitory activities with the IC_{50} values ranging from 3.17 μ M to 7.06 μ M, nearly 2~14 folds increased compared to **5a-5d**. On the contrary, compounds **5e-5f** were about 2~8 folds more active than **6e-6f**, with the IC_{50} values ranging from 2.06 μ M to 8.31 μ M. These facts clearly indicated

that when the C3' and C4' positions were substituted by OH and the C2' and C4' positions were substituted by OCH₃, the inhibitory activity can be increased.

Compounds **6a**, **6e** with OH at C6 position had similar IC₅₀ values with the compounds **6b**, **6f** which had OH at C7 position. And compounds **5c**, **5g**, **6c**, **6g**, **7c**, **7g** bearing Br at the C6 position also had similar IC₅₀ values with compounds **5d**, **5h**, **6d**, **6h**, **7d**, **7h** which Br at the C7 position except compound **5c**. These results suggested that the positions of OH and Br have no significant effect on the inhibitory activity. Interestingly, compounds **5a**, **5e**, **7a**, **7e**, which had OCH₃ at the C6 position, showed higher activities than the corresponding isomers **5b**, **5f**, **7b**, **7f** with OCH₃ at the C7 position, suggesting that OCH₃ at the C6 position could improve the inhibitory activity.

Table 1. *In vitro* α -glucosidase inhibitory activity of compounds **5a-5h**, **6a-6h**, **7a-7h**.



Compounds	R	R ₁	R ₂	R ₃	R ₄	R ₅	IC ₅₀ (μM) ^a
5a	H	OCH ₃	H	OCH ₃	OCH ₃	H	15.90±0.91
5b	H	H	OCH ₃	OCH ₃	OCH ₃	H	>100 ^b
5c	H	Br	H	OCH ₃	OCH ₃	H	11.82±0.82
5d	H	H	Br	OCH ₃	OCH ₃	H	29.84±3.47
5e	H	OCH ₃	H	OCH ₃	H	OCH ₃	2.06±0.16
5f	H	H	OCH ₃	OCH ₃	H	OCH ₃	8.31±0.88
5g	H	Br	H	OCH ₃	H	OCH ₃	2.78±0.22
5h	H	H	Br	OCH ₃	H	OCH ₃	3.07±0.56
6a	H	OH	H	OH	OH	H	6.13±0.09
6b	H	H	OH	OH	OH	H	7.06±0.89
6c	H	Br	H	OH	OH	H	5.23±0.53
6d	H	H	Br	OH	OH	H	3.17±0.61
6e	H	OH	H	OH	H	OH	17.61±1.68
6f	H	H	OH	OH	H	OH	15.62±1.13
6g	H	Br	H	OH	H	OH	5.87±0.76
6h	H	H	Br	OH	H	OH	5.88±0.32
7a	OAc	OCH ₃	H	OCH ₃	OCH ₃	H	98.63±4.12
7b	OAc	H	OCH ₃	OCH ₃	OCH ₃	H	>100 ^b
7c	OAc	Br	H	OCH ₃	OCH ₃	H	26.11±2.95
7d	OAc	H	Br	OCH ₃	OCH ₃	H	32.33±0.82
7e	OAc	OCH ₃	H	OCH ₃	H	OCH ₃	33.16±2.51
7f	OAc	H	OCH ₃	OCH ₃	H	OCH ₃	42.60±0.09
7g	OAc	Br	H	OCH ₃	H	OCH ₃	12.78±0.01
7h	OAc	H	Br	OCH ₃	H	OCH ₃	12.13±1.84

^a IC₅₀ value: concentration that inhibits the activity of α-glucosidase by 50% (mean ±SD). The IC₅₀ value of positive control (1-deoxynojirimycin, PG) is 59.50 ± 4.7 μM. The IC₅₀ value of parental compound **a** is 160.8 μM^[17], and compound **b** is 10.6 μM^[21].

^b The compounds precipitated when the concentration was higher than 100 μM, but the inhibition is lower than 50%. Therefore, the IC₅₀ value of compounds **5b** and **7b** can not be obtained.

2.3 Inhibition kinetics of α-glucosidase

To further explore the interaction mechanism of xanthone-triazole derivatives with α -glucosidase, the inhibition types of potential compounds **5e**, **5g**, **5h**, **6c**, **6d**, **6g** and **6h** were tested using Lineweaver-Burk plot analysis [37, 38]. As shown in Figure 3, the double reciprocal plots showed straight lines with the same Michaelis constant (k_m), indicating that compounds **5e**, **5g**, **5h**, **6c**, **6d**, **6g** and **6h** are noncompetitive inhibitors of α -glucosidase.

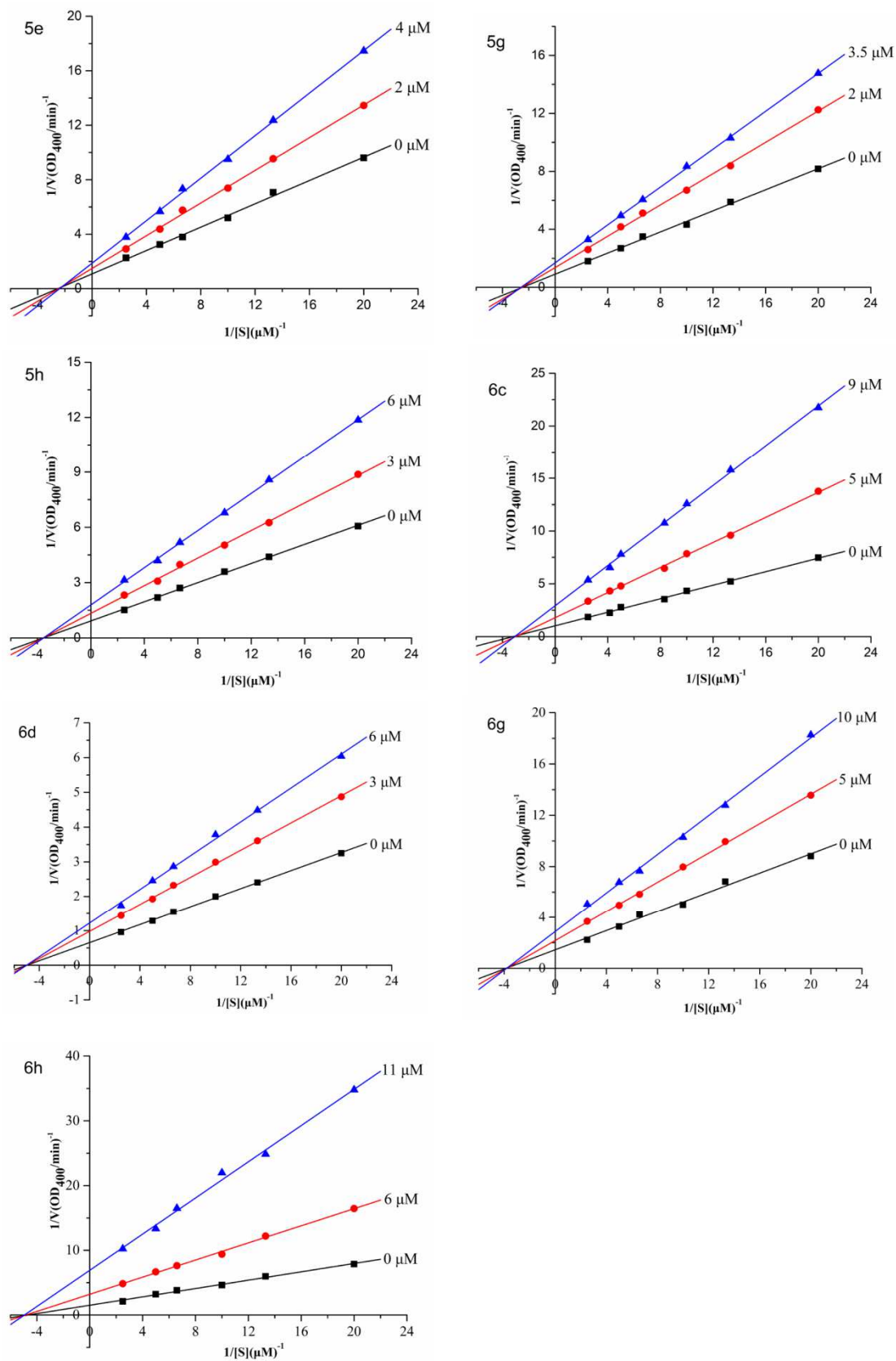


Figure 3. Lineweaver-Burk plots ($1/V$ vs $1/[S]$) of α -glucosidase inhibition of compounds 5e, 5g, 5h, 6c, 6d, 6g and 6h.

2.4 Molecular docking

To reveal the binding mode of these compounds towards α -glucosidase, molecular docking studies were performed. Compounds **5e**, **5g**, **5h**, **6c**, **6d**, **6g** and **6h** with high enzyme inhibition, were evaluated for their possible interactions with the enzyme, particularly the interactions between the triazole moiety and the enzyme. The homology model of α -glucosidase provided by SWISS-MODEL Repository was used [39], with the model quality estimation performed, due to the unavailability of the crystal structure of α -glucosidase from *Saccharomyces cerevisiae*.

From the results of the docking studies, it can be found that all of the examined compounds bind to allosteric sites away from the active site (Asp214, Glu276 and Asp349) of the enzyme (Figure 4), which was consistent with their noncompetitive property validated in the enzyme kinetic assay.

Various interactions could be found between these compounds and the allosteric sites of the enzyme. For example, hydrogen bonds could be formed between the OH and carbonyl oxygen atoms of the compounds and enzyme, and the aromatic xanthone core and the side benzene ring could also form π - π or π -cation interactions with residues of the enzyme (Figure 5: (A), (B)). Besides, the promoting effects of the triazole ring could be illustrated in that it could not only form a hydrogen bond but also participate in π - π interactions (Figure 5: (C), (D)).

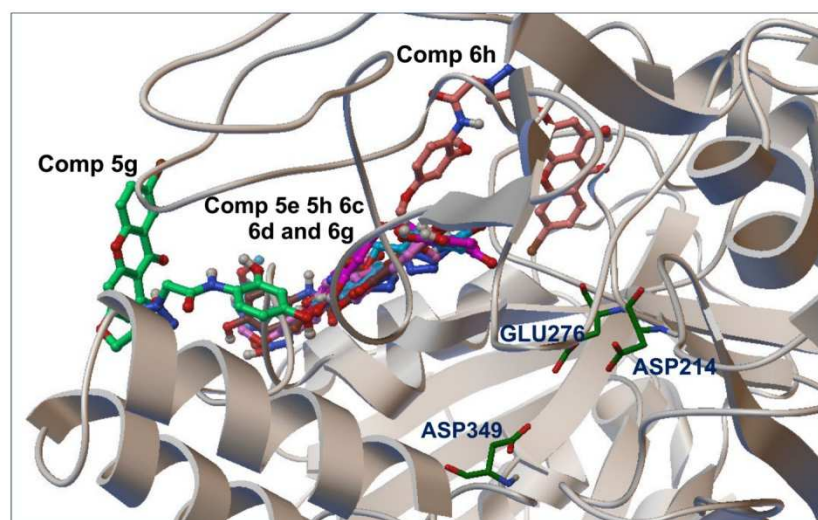


Figure 4. Binding positions of compounds **5e**, **5g**, **5h**, **6c**, **6d**, **6g** and **6h**. All the examined compounds bind to allosteric sites away from the active site (Asp214, Glu276 and Asp349) of α -glucosidase.

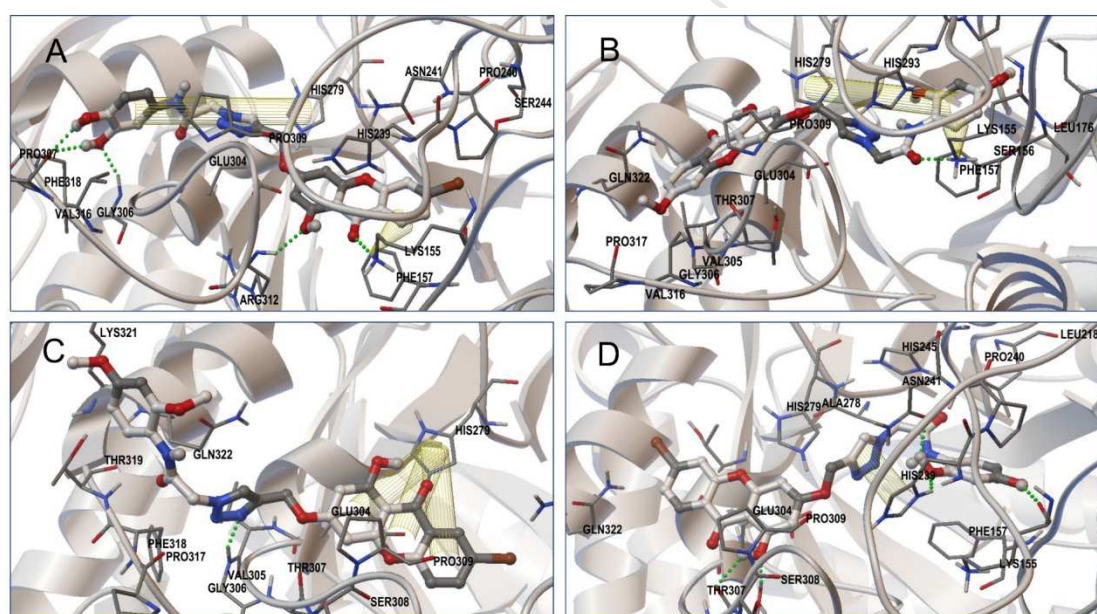


Figure 5. Predicted interactions between α -glucosidase and compounds **6c**, **5e**, **5h** and **6g**. The green dashed lines stand for hydrogen bonds, yellow columns stand for π - π interactions, and yellow cones stand for π -cation interactions. (A) Compound **6c**: Hydrogen bonds, π - π interactions, π -cation interactions. (B) Compound **5e**: Hydrogen bonds, π - π interactions, π -cation interactions. (C) Compound **5h**: Hydrogen bonds, π - π interactions. (D) Compound **6g**: Hydrogen bonds, π - π interactions.

2.5 Cytotoxicity and glucose uptake assays

2.5.1 *In vitro* cytotoxicity

Most of the drugs are metabolized in the liver, which in turn have impacts on liver function. If the drugs are toxic to the liver, it would cause liver damage. In order to determine the toxicities of the synthetic xanthone-triazole derivatives, we conducted MTT assay on human hepatocyte cell line (LO2).

As shown in Table 2, the IC₅₀ values of all the synthesized compounds exhibited more than 100 μM in the LO2 cells except **5e**, **5f**, **6g**, **7b**, **7c** and **7h**, showing that most of the compounds have low toxicity to liver in the range of tested dose.

Table 2. LO2 cytotoxicity of compounds **5a-5h**, **6a-6h**, **7a-7h**

Compounds	IC ₅₀ (μM)	Compounds	IC ₅₀ (μM)	Compounds	IC ₅₀ (μM) ^a
5a	>100	6a	>100	7a	>100
5b	>100	6b	>100	7b	24.92±2.38
5c	>100	6c	>100	7c	25.95±3.10
5d	>100	6d	>100	7d	>100
5e	89.06±4.89	6e	>100	7e	>100
5f	65.43±3.51	6f	>100	7f	>100
5g	>100	6g	73.95±6.73	7g	>100
5h	>100	6h	>100	7h	80.72±1.63

^a IC₅₀ value: concentration that inhibits cells survival by 50% (means ± SD).

Furthermore, the effects of compounds **a**, **5e**, **5f**, **5g**, **5h**, **6a**, **6b**, **6c**, **6d**, **6g**, **6h**, **7g** and **7h** at the low concentrations on HepG2 cells growth were showed in the Figure 6. It indicated that the low concentrations of compounds had no effect on cells survival, which revealed the glucose uptake assay on HepG2 cells could be performed at these concentrations.

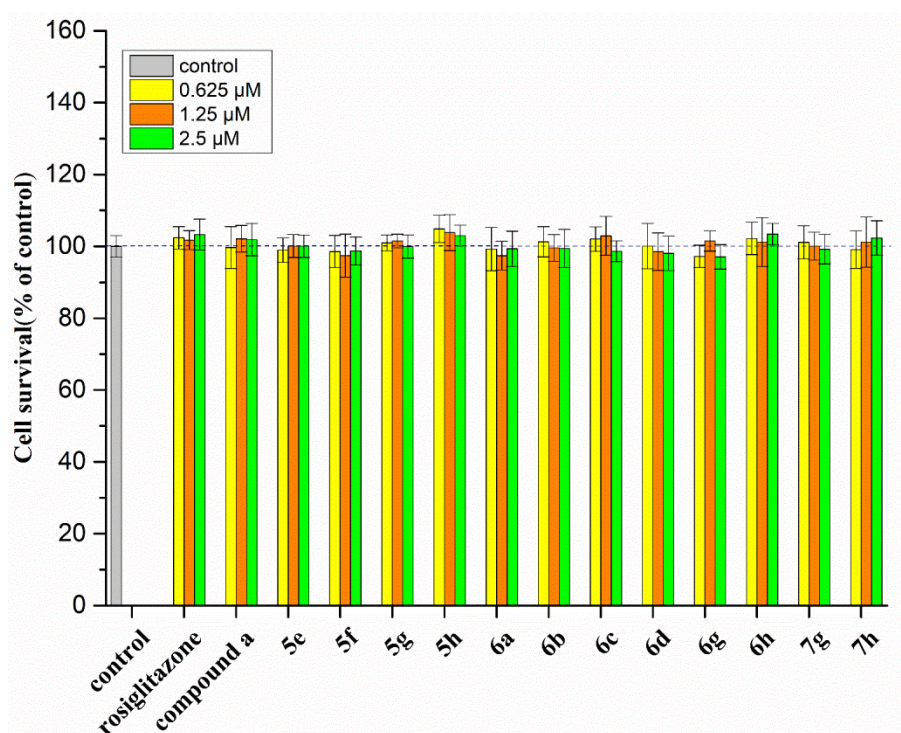


Figure 6. Effects of different concentrations of compounds **a**, **5e**, **5f**, **5g**, **5h**, **6a**, **6b**, **6c**, **6d**, **6g**, **6h**, **7g** and **7h** on HepG2 cells growth.

2.5.2 Glucose uptake in HepG2 cells

HepG2 cells maintain many functions of the human liver and have the same glycometabolic function as human hepatocytes, meanwhile, HepG2 cells are easy to cultivate and reproduce rapidly, thus it is widely used as glucose uptake model *in vitro* [12, 13, 38].

To investigate whether the xanthone-triazole derivatives had another treatment approach to type 2 diabetes, the potent α -glycosidase inhibitors were chosen to evaluate the glucose uptake in HepG2 cells at 0.625, 1.25 and 2.5 μ M. The results were shown in Figure 7. Rosiglitazone was used as positive control and parental compound **a** was also used as a reference. Rosiglitazone exerted improvement of an approximately 50 % glucose uptake in HepG2 cells compared with the control group and there is no significant difference when the concentration changed at the range of 0.625, 1.25 and 2.5 μ M. Inspiringly, the seven compounds **5e**, **5g**, **6a**, **6c**, **6d**, **6h** and **7g** significantly enhanced the glucose uptake in HepG2 cells, but the parental

compound **a** had little effect on promoting the glucose uptake. Among them, **5g**, **6d** had similar effects to rosiglitazone, and **5e**, **6a**, **6c** and **7g** displayed higher activities than rosiglitazone with concentration dependence. In particular, at 0.625, 1.25 and 2.5 μM , the most active compound **7g** increased the activity by 61 %, 90 % and 163 %, respectively, compared with the control. Besides, comparing the glucose uptake of the pair of compounds **5e/5f**, **5g/5h**, **6a/6b**, **6c/6d** and **7g/7h**, it showed that bearing a substituent such as OCH_3 , OH or Br at C6 position of the xanthone ring presented more positive effects than the substituent at C7 position.

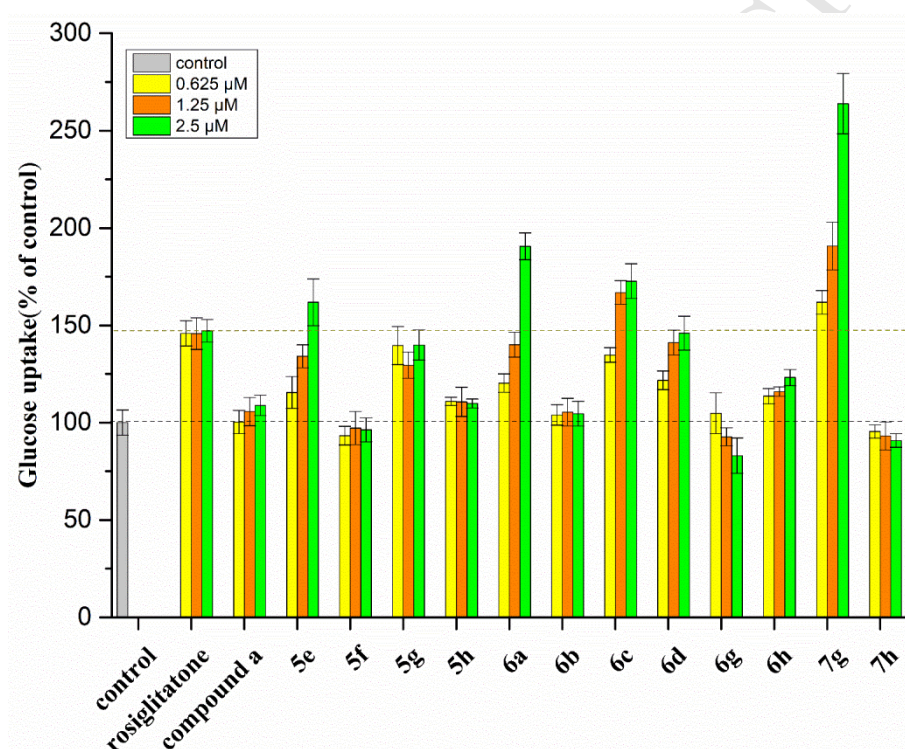


Figure 7. Effects of compounds **a**, **5e**, **5f**, **5g**, **5h**, **6a**, **6b**, **6c**, **6d**, **6g**, **6h**, **7g** and **7h** on glucose uptake of HepG2 cells.

3. Conclusion

In summary, twenty-four novel xanthone-triazole derivatives have been designed, synthesized, and their inhibitory activities of α -glucosidase, inhibition kinetics, molecular docking, cytotoxicity and glucose uptake were evaluated.

As expected, the introduction of aromatic ring substituted triazole to the C3-OH position of the parental xanthone ring enhanced the α -glucosidase inhibitory activities,

and the IC_{50} values of the most synthetic xanthone-triazole derivatives ranging from 2.06~17.61 μM , showed higher activities than 1-deoxynojirimycin. Especially, the IC_{50} value of compounds **5e**, **5g**, **5h** and **6d** were 2.06, 2.78, 3.07 and 3.17 μM , exhibiting greater inhibitory activities than the most potent reported synthetic xanthone derivatives (the IC_{50} value was 5.8 μM [18]). Docking studies reveal that the increase of the activities may due to the hydrogen bond and π - π or π -cation interaction of aromatic ring substituted triazole moiety with the enzyme.

The structure-activity relationship analysis suggests that OH at the C1 position of xanthone ring also has great influence on improving the inhibitory activity, and the different substituents at the different positions may influence the inhibition towards α -glucosidase. It may due to the chemical softness of the substituents, the hydrophobic interaction or hydrogen bonding between the compounds and the α -glucosidase.

Kinetic analysis reveals that the compounds exhibit potent inhibitory activities toward yeast's α -glucosidase via a noncompetitive mechanism, and molecular docking results consist with the results of the kinetic study that these compounds did not interact with the active site of the enzyme.

It is worth to highlight that compounds **5e**, **6a**, **6c** and **7g** showed good inhibitory effects toward α -glucosidase and high activities in promoting the glucose uptake in HepG2 cells, suggesting that these four compounds may have dual effects in the glucose levels control. Additionally, the cytotoxicity assays confirmed that most of the synthetic xanthone-triazole derivatives have low toxicity. Accordingly, these compounds may be potentially developed as antidiabetic agents for the type 2 diabetes in the future.

4. Experimental designs and methods

4.1 General

Melting points (Mp) were obtained on WRS-3 melting point instrument. Infrared (IR) spectra were collected by a Perkin-Elmer model Lambda 950-IR spectrophotometer with KBr pellets. High resolution (HR) mass spectra were measured using a Thermo LTQ Orbitrap Elite or TSQ Quantum XLS mass spectrometer. ^1H and ^{13}C NMR spectra were recorded with Bruker Avance III 400 MHz and Varian Inova 500 MHz in DMSO- d_6 or CDCl_3 . UV spectra were determined using a Shimadzu UV-3250 scanning spectrophotometer.

1-Deoxynojirimycin, rosiglitazone, α -glucosidase (from *Saccharomyces cerevisiae*), dimethylsulfoxide (DMSO) and p-nitrophenyl- α -D-glucopyranoside (PNP) were purchased from Sigma (St. Louis, MO, USA). Analytical thin-layer chromatography was performed with silica gel plates (Merck, TLC silica gel 60 F254). Column chromatography was performed with 100-200 mesh silica gel (Qingdao Haiyang Chemical Co., Ltd., China). Others commercial chemicals and solvents were of analytical grade and used without further purification. All the final compounds had a purity of > 95% determined by HPLC (Agilent 1260 LC system) on a Sapphire C_{18} column (Thermo Fisher Scientific, 4.6 mm \times 150 mm, 5 μm) or Eclipse XDB C_{18} column (Agilent Technologies, 4.6 mm \times 150 mm, 5 μm) with MeOH/ H_2O (70/30 v/v) at 1 mL/min flow rate and 254 nm detector wavelengths.

4.1.1 Compounds **1a-1d** were synthesized as previously reported [29].

4.1.2 General methods for the synthesis of **2a-2d**.

A mixture of compounds **1a-1d** (1.0 mmol), 3-Bromopropyne (1.0 mmol) and K_2CO_3 (5.0 mmol) in acetone (15 mL) was stirred at 60 $^\circ\text{C}$ for 5-14 h. The reaction mixture was filtered, and the residue was washed with CH_3OH (3 \times 10 mL). The filtrate was combined and concentrated, then the compounds **2a-2d** were obtained by flash chromatography.

4.1.3 General methods for the synthesis of **3a** and **3b**.

Chloroacetyl chloride (0.80 mL, 12.0 mmol) was added dropwise into the solution of dry THF (10 mL) containing substituted aniline (10.0 mmol) with continuous stirring to avoid the vigorous reaction at 0 °C under nitrogen atmosphere. After 1.5-2 h, the mixture was poured into 100 mL of ice water, and extracted with DCM (2 × 300 mL). The collected organic layers were dried over Na₂SO₄ and the solvent was evaporated under reduced pressure to obtain the products **3a** and **3b**, which were pure enough without further purification.

4.1.4 General methods for the synthesis of **4a** and **4b**.

A solution of NaN₃ (12.0 mmol) in DMF (20 mL) was added **3a** or **3b** (4.0 mmol), and the reaction mixture was stirred at room temperature for 4 h. Water (200 mL) was carefully added to the reaction mixture. Then, the aqueous layer was extracted with CH₂Cl₂ (2 × 200 mL). The collected organic layers were washed with water (500 mL) and dried over Na₂SO₄. The drying agent was filtered out and concentrated. Concentrated product was purified by flash chromatography.

4.1.5 General methods for the synthesis of **5a-5h**.

The corresponding xanthone derivatives **2a-2d** (1.0 mmol) were reacted with **4a** or **4b** (1.0 mmol) at room temperature overnight in the presence of CuSO₄·5H₂O (0.1 mmol), sodium ascorbate (0.2 mmol) using DMF (10 mL) as a solvent. Then the solution was poured into ice water (100 mL), the obtained precipitate was filtered and dried, purified by flash chromatography to obtain **5a-5h** respectively.

4.1.5.1.

N-(3,4-dimethoxyphenyl)-2-(4-(((1-hydroxy-6-methoxy-9-oxo-9H-xanthen-3-yl)oxy)methyl)-1H-1,2,3-triazol-1-yl)acetamide (**5a**). White solid; Yield 84.9 %; Mp; 245-246 °C; Purity 97.5 %; IR (KBr): 3446, 3250, 3144, 3079, 2938, 2833, 1663, 1604, 1565, 1511, 1456, 1404, 1369, 1306, 1267, 1242, 1210, 1154, 1103, 1080, 1018, 973, 940, 814, 671, 642, 556 cm⁻¹; ¹H NMR (400 MHz, DMSO-*d*₆) δ 12.95 (s, 1H), 10.37 (s, 1H), 8.33 (s, 1H), 8.02 (d, *J* = 8.8 Hz, 1H), 7.30 (s, 1H), 7.16 - 6.97 (m, 3H),

6.90 (d, $J = 8.7$ Hz, 1H), 6.71 (s, 1H), 6.51 (s, 1H), 5.33 (s, 4H), 3.92 (s, 3H), 3.71 (s, 6H); ^{13}C NMR (100 MHz, DMSO- d_6) δ 179.35, 165.30, 164.82, 163.65, 162.61, 157.51, 157.15, 148.57, 145.15, 141.54, 131.91, 126.81, 126.74, 113.66, 113.33, 112.04, 111.10, 104.25, 102.82, 100.48, 97.58, 93.46, 61.82, 56.22, 55.65, 55.30, 52.21; HRMS (ESI) calcd for $\text{C}_{27}\text{H}_{23}\text{O}_8\text{N}_4$ $[\text{M}-\text{H}]^-$: $m/z = 531.15213$, found 531.15223.

4.1.5.2.

N-(3,4-dimethoxyphenyl)-2-(4-(((1-hydroxy-7-methoxy-9-oxo-9H-xanthen-3-yl)oxy)methyl)-1H-1,2,3-triazol-1-yl)acetamide (**5b**). Yellow solid; Yield 81.3 %; Mp 204-205 °C. Purity 99.8 %; IR (KBr): 3564, 3261, 3141, 3073, 2964, 2933, 2833, 1667, 1603, 1576, 1513, 1489, 1436, 1404, 1368, 1339, 1297, 1265, 1237, 1215, 1160, 1129, 1082, 1029, 970, 837, 814, 768, 692, 559 cm^{-1} ; ^1H NMR (400 MHz, DMSO- d_6) δ 12.81 (s, 1H), 10.37 (s, 1H), 8.33 (s, 1H), 7.55 (d, $J = 8.6$ Hz, 1H), 7.51 - 7.40 (m, 2H), 7.30 (s, 1H), 7.05 (d, $J = 8.7$ Hz, 1H), 6.90 (d, $J = 8.7$ Hz, 1H), 6.76 (s, 1H), 6.50 (s, 1H), 5.34 (s, 4H), 3.86 (s, 3H), 3.71 (s, 6H); ^{13}C NMR (100 MHz, DMSO- d_6) δ 179.82, 165.14, 163.65, 162.42, 157.20, 155.75, 150.13, 148.56, 145.15, 141.51, 131.91, 126.75, 124.82, 120.16, 119.27, 112.03, 111.10, 105.18, 104.25, 102.96, 97.58, 93.24, 61.84, 55.75, 55.65, 55.30, 52.21; HRMS (ESI) calcd for $\text{C}_{27}\text{H}_{23}\text{O}_8\text{N}_4$ $[\text{M}-\text{H}]^-$: $m/z = 531.15213$, found 531.15217.

4.1.5.3.

2-(4-(((6-bromo-1-hydroxy-9-oxo-9H-xanthen-3-yl)oxy)methyl)-1H-1,2,3-triazol-1-yl)-*N*-(3,4-dimethoxyphenyl)acetamide (**5c**). Yellow solid; Yield 76.3 %; Mp 254-256 °C; Purity 97.2 %; IR (KBr): 3465, 3285, 3069, 2941, 2836, 1657, 1598, 1556, 1515, 1447, 1424, 1372, 1312, 1287, 1229, 1164, 1061, 1024, 924, 882, 818, 796, 663, 553 cm^{-1} ; ^1H NMR (400 MHz, DMSO- d_6) δ 12.62 (s, 1H), 10.37 (s, 1H), 8.33 (s, 1H), 8.02 (d, $J = 8.5$ Hz, 1H), 7.90 (d, $J = 1.7$ Hz, 1H), 7.64 (dd, $J = 8.5, 1.7$ Hz, 1H), 7.30 (d, $J = 2.4$ Hz, 1H), 7.05 (dd, $J = 8.6, 2.4$ Hz, 1H), 6.90 (d, $J = 8.6$ Hz, 1H), 6.76 (d, $J = 2.3$ Hz, 1H), 6.55 (d, $J = 2.3$ Hz, 1H), 5.34 (d, $J = 5.2$ Hz, 4H), 3.71

(s, 6H); ^{13}C NMR (100 MHz, DMSO- d_6) δ 179.39, 165.46, 163.57, 162.51, 156.96, 155.53, 148.57, 145.17, 141.43, 131.88, 128.98, 127.78, 126.96, 126.67, 120.50, 119.03, 112.10, 111.14, 104.36, 103.22, 97.97, 93.67, 61.93, 55.67, 55.31, 52.19; HRMS (ESI) calcd for $\text{C}_{26}\text{H}_{20}\text{O}_7\text{N}_4\text{Br}$ [M-H] $^-$: $m/z = 579.05208$, found 579.05223.

4.1.5.4.

2-(4-(((7-bromo-1-hydroxy-9-oxo-9H-xanthen-3-yl)oxy)methyl)-1H-1,2,3-triazol-1-yl)-N-(3,4-dimethoxyphenyl)acetamide (**5d**). Yellow solid; Yield 71.8 %; Mp 236-239 $^\circ\text{C}$; Purity 97.7 %; IR (KBr): 3460, 3264, 3088, 2924, 2836, 1658, 1601, 1561, 1515, 1461, 1412, 1368, 1306, 1277, 1228, 1162, 1129, 1075, 1022, 969, 830, 807, 713, 645, 553 cm^{-1} ; ^1H NMR (400 MHz, DMSO- d_6) δ 12.54 (s, 1H), 10.37 (s, 1H), 8.33 (s, 1H), 8.17 (d, $J = 2.5$ Hz, 1H), 8.01 (dd, $J = 8.9, 2.5$ Hz, 1H), 7.60 (d, $J = 8.9$ Hz, 1H), 7.30 (d, $J = 2.3$ Hz, 1H), 7.05 (dd, $J = 8.7, 2.3$ Hz, 1H), 6.90 (d, $J = 8.7$ Hz, 1H), 6.81 (d, $J = 2.2$ Hz, 1H), 6.56 (d, $J = 2.2$ Hz, 1H), 5.34 (d, $J = 7.4$ Hz, 4H), 3.71 (d, $J = 2.9$ Hz, 6H); ^{13}C NMR (100 MHz, DMSO- d_6) δ 178.87, 165.60, 163.63, 162.50, 157.12, 154.45, 148.55, 145.14, 141.41, 138.29, 131.91, 127.25, 126.80, 121.49, 120.39, 116.57, 112.03, 111.09, 104.24, 103.23, 97.99, 93.78, 61.95, 55.65, 55.30, 52.20; HRMS (ESI) calcd for $\text{C}_{26}\text{H}_{20}\text{O}_7\text{N}_4\text{Br}$ [M-H] $^-$: $m/z = 579.05208$, found 579.05159.

4.1.5.5.

N-(2,4-dimethoxyphenyl)-2-(4-(((1-hydroxy-6-methoxy-9-oxo-9H-xanthen-3-yl)oxy)methyl)-1H-1,2,3-triazol-1-yl)acetamide (**5e**). White solid; Yield 86.2 %; Mp 253-260 $^\circ\text{C}$; Purity 95.9 %; IR (KBr): 3266, 3066, 3011, 2943, 2833, 1664, 1602, 1561, 1503, 1445, 1362, 1307, 1269, 1211, 1158, 1107, 1080, 1018, 968, 916, 827, 799, 726, 672, 641, 561, 517 cm^{-1} ; ^1H NMR (400 MHz, DMSO- d_6) δ 12.96 (s, 1H), 9.64 (s, 1H), 8.30 (s, 1H), 8.04 (d, $J = 8.9$ Hz, 1H), 7.70 (d, $J = 8.7$ Hz, 1H), 7.12 (d, $J = 2.3$ Hz, 1H), 7.05 (dd, $J = 8.9, 2.3$ Hz, 1H), 6.73 (d, $J = 2.2$ Hz, 1H), 6.64 (d, $J = 2.6$ Hz, 1H), 6.52 (d, $J = 2.2$ Hz, 1H), 6.48 (dd, $J = 8.7, 2.6$ Hz, 1H), 5.41 (s, 2H), 5.33 (s, 2H), 3.92 (s, 3H), 3.84 (s, 3H), 3.74 (s, 3H); ^{13}C NMR (100 MHz, DMSO- d_6) δ

179.41, 165.36, 164.87, 164.07, 162.64, 157.58, 157.20, 157.05, 151.34, 141.51, 126.87, 126.75, 123.37, 119.55, 113.74, 113.37, 104.10, 102.86, 100.55, 98.90, 97.62, 93.51, 61.84, 56.28, 55.77, 55.31, 52.11; HRMS (ESI) calcd for C₂₇H₂₃O₈N₄ [M-H]⁻: m/z = 531.15213, found 531.15216.

4.1.5.6.

N-(2,4-dimethoxyphenyl)-2-(4-(((1-hydroxy-7-methoxy-9-oxo-9H-xanthen-3-yl)oxy)methyl)-1H-1,2,3-triazol-1-yl)acetamide (**5f**). Yellow solid; Yield 83.8 %; Mp 235-237 °C; Purity 96.4 %; IR(KBr): 3270, 3139, 3086, 3006, 2959, 2836, 1659, 1607, 1577, 1545, 1485, 1466, 1434, 1406, 1367, 1308, 1284, 1237, 1208, 1152, 1125, 1081, 1030, 966, 937, 825, 784, 712, 590, 509 cm⁻¹; ¹H NMR (400 MHz, DMSO-*d*₆) δ 12.81 (s, 1H), 9.63 (s, 1H), 8.31 (s, 1H), 7.71 (d, *J* = 8.8 Hz, 1H), 7.56 (d, *J* = 8.8 Hz, 1H), 7.50 - 7.39 (m, 2H), 6.75 (d, *J* = 2.2 Hz, 1H), 6.63 (d, *J* = 2.6 Hz, 1H), 6.55 - 6.40 (m, 2H), 5.42 (s, 2H), 5.33 (s, 2H), 3.85 (d, *J* = 8.0 Hz, 6H), 3.74 (s, 3H); ¹³C NMR (100 MHz, DMSO-*d*₆) δ 179.83, 165.15, 164.05, 162.42, 157.20, 157.03, 155.75, 151.31, 150.14, 141.49, 126.75, 124.83, 123.33, 120.16, 119.55, 119.29, 105.18, 104.08, 102.96, 98.88, 97.58, 93.25, 61.85, 55.76 (2C), 55.29, 52.11; HRMS (ESI) calcd for C₂₇H₂₃O₈N₄ [M-H]⁻: m/z = 531.15213, found 531.15233.

4.1.5.7.

2-(4-(((6-bromo-1-hydroxy-9-oxo-9H-xanthen-3-yl)oxy)methyl)-1H-1,2,3-triazol-1-yl)-N-(2,4-dimethoxyphenyl)acetamide (**5g**). Yellow solid; Yield 70.5 %; Mp 244-246 °C; Purity 97.5 %; IR(KBr): 3293, 3063, 2935, 2833, 1656, 1597, 1543, 1504, 1449, 1422, 1373, 1310, 1282, 1207, 1161, 1126, 1081, 1062, 1036, 966, 923, 890, 821, 794, 662, 574, 511 cm⁻¹; ¹H NMR (400 MHz, DMSO-*d*₆) δ 12.63 (s, 1H), 9.62 (s, 1H), 8.30 (s, 1H), 8.03 (d, *J* = 8.6 Hz, 1H), 7.91 (d, *J* = 1.9 Hz, 1H), 7.70 (d, *J* = 8.8 Hz, 1H), 7.65 (dd, *J* = 8.6, 1.9 Hz, 1H), 6.76 (d, *J* = 2.3 Hz, 1H), 6.63 (d, *J* = 2.7 Hz, 1H), 6.55 (d, *J* = 2.3 Hz, 1H), 6.47 (dd, *J* = 8.8, 2.7 Hz, 1H), 5.41 (s, 2H), 5.35 (s, 2H), 3.84 (s, 3H), 3.74 (s, 3H); ¹³C NMR (125 MHz, DMSO-*d*₆) δ 179.66, 165.58, 164.10, 162.62, 157.16, 157.07, 155.76, 151.36, 141.44, 129.16, 127.98, 127.18, 126.86,

123.40, 120.72, 119.55, 119.24, 104.11, 103.39, 98.91, 98.09, 93.83, 61.98, 55.80, 55.34, 52.13; HRMS (ESI) calcd for $C_{26}H_{20}O_7N_4Br$ $[M-H]^-$: $m/z = 579.05208$, found 579.05188.

4.1.5.8.

2-(4-(((7-bromo-1-hydroxy-9-oxo-9H-xanthen-3-yl)oxy)methyl)-1H-1,2,3-triazol-1-yl)-N-(2,4-dimethoxyphenyl)acetamide (**5h**). White solid; Yield 88.6 %; Mp 245-248 °C; Purity 97.9 %; IR(KBr): 3250, 3214, 3072, 3002, 2961, 2936, 2833, 1658, 1602, 1557, 1508, 1461, 1414, 1370, 1331, 1305, 1281, 1206, 1163, 1128, 1077, 1040, 968, 819, 715, 649, 580, 517 cm^{-1} ; 1H NMR (500 MHz, DMSO- d_6) δ 12.54 (s, 1H), 9.63 (s, 1H), 8.31 (s, 1H), 8.18 (d, $J = 2.6$ Hz, 1H), 8.01 (dd, $J = 9.0, 2.6$ Hz, 1H), 7.70 (d, $J = 8.9$ Hz, 1H), 7.61 (d, $J = 9.0$ Hz, 1H), 6.82 (d, $J = 2.3$ Hz, 1H), 6.64 (d, $J = 2.7$ Hz, 1H), 6.56 (d, $J = 2.3$ Hz, 1H), 6.47 (dd, $J = 8.9, 2.7$ Hz, 1H), 5.41 (s, 2H), 5.35 (s, 2H), 3.84 (s, 3H), 3.74 (s, 3H); ^{13}C NMR (125 MHz, DMSO- d_6) δ 178.97, 165.63, 164.06, 162.53, 157.19, 157.05, 154.53, 151.34, 141.39, 138.35, 127.31, 126.80, 123.36, 121.58, 120.48, 119.53, 116.59, 104.10, 103.30, 98.90, 98.04, 93.84, 61.96, 55.77, 55.31, 52.10; HRMS (ESI) calcd for $C_{26}H_{20}O_7N_4Br$ $[M-H]^-$: $m/z = 579.05208$, found 579.05194.

4.1.6 General methods for the synthesis of **6a-6h**.

A solution of **5a-5h** (0.5 mmol) in dry CH_2Cl_2 (30 mL) was added BBr_3 (4.7 mL, 50 mmol) slowly through the septum with stirring at 0 °C. After 0.5 h, the solution was stirred for 24-72 h at room temperature, the mixture was poured into ice water (300 mL) and stirred for 0.5 h. Solid was precipitated. After being filtered and dried, the solid was purified by flash chromatography to obtain **6a-6h**, respectively.

4.1.6.1.

2-(4-(((1,6-dihydroxy-9-oxo-9H-xanthen-3-yl)oxy)methyl)-1H-1,2,3-triazol-1-yl)-N-(3,4-dihydroxyphenyl)acetamide (**6a**). White solid; Yield 29.5 %; Mp 294-296 °C; Purity 95.5 %; IR(KBr): 3496, 3415, 3255, 3139, 3084, 2705, 2583, 1665, 1608, 1578, 1509, 1462, 1389, 1296, 1252, 1180, 1145, 1109, 1086, 965, 924, 823, 726, 668, 564,

530, 454 cm^{-1} ; ^1H NMR (400 MHz, $\text{DMSO-}d_6$) δ 13.05 (s, 1H), 11.10 (s, 1H), 10.13 (s, 1H), 9.01 (s, 1H), 8.69 (s, 1H), 8.30 (s, 1H), 7.99 (d, $J = 8.8$ Hz, 1H), 7.09 (d, $J = 2.4$ Hz, 1H), 6.92 (dd, $J = 8.8, 2.1$ Hz, 1H), 6.87 - 6.78 (m, 2H), 6.74 (d, $J = 2.3$ Hz, 1H), 6.65 (d, $J = 8.5$ Hz, 1H), 6.48 (d, $J = 2.3$ Hz, 1H), 5.30 (d, $J = 11.8$ Hz, 4H); ^{13}C NMR (100 MHz, $\text{DMSO-}d_6$) δ 179.35, 164.71, 164.50, 163.19, 162.58, 157.58, 157.18, 145.07, 141.76, 141.54, 130.38, 127.30, 126.66, 115.37, 114.26, 112.35, 110.46, 107.90, 102.73, 102.05, 97.55, 93.41, 61.79, 52.23; HRMS (ESI) calcd for $\text{C}_{24}\text{H}_{17}\text{O}_8\text{N}_4$ $[\text{M-H}]^-$: $m/z = 489.10519$, found 489.10528.

4.1.6.2.

2-(4-(((1,7-dihydroxy-9-oxo-9H-xanthen-3-yl)oxy)methyl)-1H-1,2,3-triazol-1-yl)-N-(3,4-dihydroxyphenyl)acetamide (**6b**); White solid; Yield 36.7 %, Mp 226-229 $^\circ\text{C}$; Purity 97.4 %; IR(KBr): 3271, 3146, 3083, 2945, 2734, 1652, 1611, 1582, 1513, 1478, 1364, 1328, 1299, 1271, 1240, 1215, 1166, 1112, 1081, 981, 818, 798, 715, 644, 594, 566, 446 cm^{-1} ; ^1H NMR (400 MHz, $\text{DMSO-}d_6$) δ 12.88 (s, 1H), 10.14 (s, 1H), 10.05 (s, 1H), 9.03 (s, 1H), 8.71 (s, 1H), 8.31 (s, 1H), 7.51 (d, $J = 9.0$ Hz, 1H), 7.42 (d, $J = 2.9$ Hz, 1H), 7.32 (dd, $J = 9.0, 2.9$ Hz, 1H), 7.09 (s, 1H), 6.84 - 6.75 (m, 2H), 6.65 (d, $J = 8.5$ Hz, 1H), 6.49 (s, 1H), 5.31 (d, $J = 17.7$ Hz, 4H); ^{13}C NMR (100 MHz, $\text{DMSO-}d_6$) δ 179.54, 165.53, 163.18, 162.57, 157.05, 155.64, 145.07, 141.76, 141.41, 130.38, 129.08, 127.88, 127.07, 126.73, 120.61, 119.13, 115.36, 110.44, 107.88, 103.30, 98.02, 93.74, 61.96, 52.23; HRMS (ESI) calcd for $\text{C}_{24}\text{H}_{17}\text{O}_8\text{N}_4$ $[\text{M-H}]^-$: $m/z = 489.10519$, found 489.10522.

4.1.6.3.

2-(4-(((6-bromo-1-hydroxy-9-oxo-9H-xanthen-3-yl)oxy)methyl)-1H-1,2,3-triazol-1-yl)-N-(3,4-dihydroxyphenyl)acetamide (**6c**); White solid; Yield 21.7 %; Mp 280-281 $^\circ\text{C}$; Purity 95.9 %; IR(KBr): 3270, 3070, 2927, 1658, 1598, 1559, 1516, 1428, 1373, 1310, 1286, 1226, 1203, 1166, 1109, 1062, 966, 926, 817, 793, 668, 577 cm^{-1} ; ^1H NMR (400 MHz, $\text{DMSO-}d_6$) δ 12.63 (s, 1H), 10.13 (s, 1H), 9.02 (s, 1H), 8.70 (s, 1H), 8.31 (s, 1H), 8.03 (d, $J = 8.4$ Hz, 1H), 7.92 (d, $J = 1.8$ Hz, 1H), 7.65 (dd, $J = 8.4, 1.8$ Hz,

1H), 7.08 (d, $J = 2.4$ Hz, 1H), 6.81 (dd, $J = 8.5, 2.4$ Hz, 1H), 6.76 (d, $J = 2.2$ Hz, 1H), 6.65 (d, $J = 8.5$ Hz, 1H), 6.55 (d, $J = 2.2$ Hz, 1H), 5.35 (s, 2H), 5.29 (s, 2H); ^{13}C NMR (100 MHz, DMSO- d_6) δ 180.08, 165.10, 163.19, 162.47, 157.34, 154.09, 149.13, 145.07, 141.76, 141.50, 130.38, 126.69, 124.82, 120.42, 119.07, 115.37, 110.45, 107.96, 107.89, 102.98, 97.44, 93.19, 61.83, 52.22; HRMS (ESI) calcd for $\text{C}_{24}\text{H}_{16}\text{O}_7\text{N}_4\text{Br}$ $[\text{M}-\text{H}]^-$: $m/z = 551.02078$, found 551.02144.

4.1.6.4.

2-(4-(((7-bromo-1-hydroxy-9-oxo-9H-xanthen-3-yl)oxy)methyl)-1H-1,2,3-triazol-1-yl)-N-(3,4-dihydroxyphenyl)acetamide (**6d**); White solid; Yield 24.5 %; Mp 265-269 °C; Purity 95.4 %; IR(KBr): 3499, 3270, 3235, 3091, 2925, 1659, 1600, 1562, 1530, 1463, 1370, 1305, 1276, 1228, 1204, 1167, 1106, 1077, 1057, 957, 817, 714, 653, 563, 532 cm^{-1} ; ^1H NMR (400 MHz, DMSO- d_6) δ 12.52 (s, 1H), 10.14 (s, 1H), 9.02 (s, 1H), 8.70 (s, 1H), 8.32 (s, 1H), 8.14 (d, $J = 2.5$ Hz, 1H), 7.99 (dd, $J = 8.9, 2.5$ Hz, 1H), 7.58 (d, $J = 8.9$ Hz, 1H), 7.08 (d, $J = 2.6$ Hz, 1H), 6.87-6.75 (m, 2H), 6.65 (d, $J = 8.5$ Hz, 1H), 6.53 (d, $J = 2.2$ Hz, 1H), 5.32 (d, $J = 20.3$ Hz, 4H); ^{13}C NMR (100 MHz, DMSO- d_6) δ 178.83, 165.59, 163.18, 162.49, 157.09, 154.42, 145.06, 141.76, 141.39, 138.27, 130.38, 127.23, 126.74, 121.44, 120.37, 116.57, 115.36, 110.45, 107.89, 103.20, 97.97, 93.75, 61.96, 52.23; HRMS (ESI) calcd for $\text{C}_{24}\text{H}_{16}\text{O}_7\text{N}_4\text{Br}$ $[\text{M}-\text{H}]^-$: $m/z = 551.02078$, found 551.02131.

4.1.6.5.

2-(4-(((1,6-dihydroxy-9-oxo-9H-xanthen-3-yl)oxy)methyl)-1H-1,2,3-triazol-1-yl)-N-(2,4-dihydroxyphenyl)acetamide (**6e**); White solid; Yield 35.2 %; Mp 290-292 °C; Purity 99.5 %; IR(KBr): 3441, 3284, 3138, 3086, 2927, 2703, 2584, 1663, 1608, 1580, 1547, 1508, 1455, 1394, 1367, 1300, 1257, 1236, 1178, 1143, 1088, 1036, 977, 923, 886, 841, 820, 725, 671, 597, 560, 534, 498 cm^{-1} ; ^1H NMR (400 MHz, DMSO- d_6) δ 13.05 (s, 1H), 11.09 (s, 1H), 9.66 (s, 1H), 9.49 (s, 1H), 9.17 (s, 1H), 8.29 (s, 1H), 7.99 (d, $J = 8.7$ Hz, 1H), 7.43 (d, $J = 8.6$ Hz, 1H), 6.91 (dd, $J = 8.7, 2.2$ Hz, 1H), 6.84 (d, $J = 2.2$ Hz, 1H), 6.74 (d, $J = 2.3$ Hz, 1H), 6.48 (d, $J = 2.3$ Hz, 1H), 6.35 (d, $J = 2.6$ Hz,

1H), 6.17 (dd, $J = 8.6, 2.6$ Hz, 1H), 5.37 (s, 2H), 5.31 (s, 2H); ^{13}C NMR (100 MHz, DMSO- d_6) δ 179.34, 164.71, 164.48, 163.88, 162.58, 157.58, 157.18, 155.09, 149.69, 141.52, 127.29, 126.65, 124.02, 116.99, 114.25, 112.35, 105.64, 102.73, 102.68, 102.05, 97.54, 93.40, 61.79, 52.09; HRMS (ESI) calcd for $\text{C}_{24}\text{H}_{17}\text{O}_8\text{N}_4$ $[\text{M-H}]^-$: $m/z = 489.10519$, found 489.10536.

4.1.6.6.

2-(4-(((1,7-dihydroxy-9-oxo-9H-xanthen-3-yl)oxy)methyl)-1H-1,2,3-triazol-1-yl)-N-(2,4-dihydroxyphenyl)acetamide (**6f**); White solid; Yield 30.2 %; Mp 266-267 °C; Purity 98.7 %; IR(KBr): 3286, 3133, 1656, 1607, 1577, 1479, 1413, 1389, 1328, 1300, 1232, 1155, 1109, 1082, 1058, 1026, 972, 951, 872, 825, 793, 713, 592, 546, 493 cm^{-1} ; ^1H NMR (400 MHz, DMSO- d_6) δ 12.87 (s, 1H), 10.06 (s, 1H), 9.69 (s, 1H), 9.51 (s, 1H), 9.19 (s, 1H), 8.30 (s, 1H), 7.49 (d, $J = 9.0$ Hz, 1H), 7.45-7.39 (m, 2H), 7.31 (dd, $J = 9.0, 3.1$ Hz, 1H), 6.75 (d, $J = 2.3$ Hz, 1H), 6.48 (d, $J = 2.3$ Hz, 1H), 6.36 (d, $J = 2.6$ Hz, 1H), 6.16 (dd, $J = 8.4, 2.6$ Hz, 1H), 5.35 (d, $J = 22.7$ Hz, 4H); ^{13}C NMR (100 MHz, DMSO- d_6) δ 180.09, 165.10, 163.90, 162.48, 157.34, 155.11, 154.10, 149.71, 149.13, 141.50, 126.72, 124.82, 124.03, 120.42, 119.07, 117.01, 107.97, 105.63, 102.98, 102.70, 97.44, 93.18, 61.84, 52.11; HRMS (ESI) calcd for $\text{C}_{24}\text{H}_{17}\text{O}_8\text{N}_4$ $[\text{M-H}]^-$: $m/z = 489.10519$, found 489.10493.

4.1.6.7.

2-(4-(((6-bromo-1-hydroxy-9-oxo-9H-xanthen-3-yl)oxy)methyl)-1H-1,2,3-triazol-1-yl)-N-(2,4-dihydroxyphenyl)acetamide (**6g**); White solid; Yield 27.2 %; Mp 264-267 °C; Purity 98.8 %; IR(KBr): 3268, 3141, 3071, 2956, 1658, 1598, 1555, 1498, 1458, 1434, 1403, 1301, 1201, 1150, 1112, 1064, 974, 922, 872, 845, 819, 671, 608, 557, 496 cm^{-1} ; ^1H NMR (400 MHz, DMSO- d_6) δ 12.61 (s, 1H), 9.67 (s, 1H), 9.49 (s, 1H), 9.17 (s, 1H), 8.30 (s, 1H), 8.01 (d, $J = 8.4$ Hz, 1H), 7.89 (s, 1H), 7.63 (d, $J = 8.4$ Hz, 1H), 7.42 (d, $J = 8.7$ Hz, 1H), 6.74 (s, 1H), 6.53 (s, 1H), 6.35 (d, $J = 2.7$ Hz, 1H), 6.16 (dd, $J = 8.7, 2.7$ Hz, 1H), 5.36 (d, $J = 16.3$ Hz, 4H); ^{13}C NMR (100 MHz, DMSO- d_6) δ 179.50, 165.52, 163.90, 162.57, 157.03, 155.62, 155.12, 149.72, 141.43, 129.09, 127.87,

127.04, 126.73, 124.05, 120.60, 119.10, 117.01, 105.66, 103.28, 102.71, 98.03, 93.73, 61.98, 52.12; HRMS (ESI) calcd for $C_{24}H_{16}O_7N_4Br$ $[M-H]^-$: $m/z = 551.02078$, found 551.02115.

4.1.6.8.

2-(4-(((7-bromo-1-hydroxy-9-oxo-9H-xanthen-3-yl)oxy)methyl)-1H-1,2,3-triazol-1-yl)-N-(2,4-dihydroxyphenyl)acetamide (**6h**); White solid; Yield 45.0 %; Mp 282-284 °C; Purity 96.3 %; IR(KBr): 3373, 3103, 2995, 2883, 2719, 1659, 1601, 1560, 1511, 1460, 1371, 1330, 1282, 1228, 1165, 1109, 1078, 1049, 976, 816, 728, 658, 569, 525, 462 cm^{-1} ; 1H NMR (400 MHz, $DMSO-d_6$) δ 12.53 (s, 1H), 9.68 (s, 1H), 9.50 (s, 1H), 9.18 (s, 1H), 8.31 (s, 1H), 8.16 (s, 1H), 8.00 (d, $J = 8.9$ Hz, 1H), 7.59 (d, $J = 8.9$ Hz, 1H), 7.43 (d, $J = 8.6$ Hz, 1H), 6.80 (s, 1H), 6.55 (s, 1H), 6.35 (s, 1H), 6.17 (d, $J = 8.6$ Hz, 1H), 5.36 (d, $J = 15.2$ Hz, 4H); ^{13}C NMR (100 MHz, $DMSO-d_6$) δ 178.85, 165.60, 163.86, 162.49, 157.11, 155.09, 154.44, 149.68, 141.37, 138.27, 127.24, 126.73, 124.01, 121.47, 120.38, 116.99, 116.56, 105.61, 103.21, 102.66, 97.98, 93.76, 61.96, 52.09; HRMS (ESI) calcd for $C_{24}H_{16}O_7N_4Br$ $[M-H]^-$: $m/z = 551.02078$, found 551.02103.

4.1.7 General methods for the synthesis of **7a-7h**.

5a-5h (0.5 mmol) and NaOAc (10.0 mmol) were added to Ac_2O (15 mL) at 90 °C for 5h. On completion, solvent was evaporated under reduced pressure, the residue was washed with water (200 mL) and dried. After that, the residue was purified by flash chromatography to give **7a-h**, respectively.

4.1.7.1.

3-(((1-(2-((3,4-dimethoxyphenyl)amino)-2-oxoethyl)-1H-1,2,3-triazol-4-yl)methoxy)-6-methoxy-9-oxo-9H-xanthen-1-yl) acetate (**7a**); White solid; Yield 86.2 %; Mp 162-164 °C; Purity 98.8 %; IR(KBr): 3506, 3265, 3144, 3076, 2938, 2833, 1769, 1659, 1613, 1562, 1514, 1435, 1364, 1264, 1233, 1200, 1171, 1143, 1064, 1023, 842, 662, 550, 459 cm^{-1} ; 1H NMR (400 MHz, $DMSO-d_6$) δ 10.38 (s, 1H), 8.34 (s, 1H), 8.00 (d, $J = 8.8$ Hz, 1H), 7.30 (d, $J = 2.2$ Hz, 1H), 7.24 (d, $J = 2.4$ Hz, 1H), 7.20 - 7.03 (m, 3H),

6.91 (d, $J = 8.7$ Hz, 1H), 6.86 (d, $J = 2.4$ Hz, 1H), 5.37 (d, $J = 19.4$ Hz, 4H), 3.91 (s, 3H), 3.71 (s, 6H), 2.36 (s, 3H); ^{13}C NMR (100 MHz, $\text{DMSO-}d_6$) δ 172.93, 168.92, 164.63, 163.66, 162.61, 158.16, 156.66, 151.03, 148.58, 145.17, 141.40, 131.92, 127.41, 126.90, 115.22, 113.54, 112.05, 111.12, 108.56, 107.75, 104.27, 100.25, 99.96, 62.02, 56.14, 55.67, 55.32, 52.23, 21.04; HRMS (ESI) calcd for $\text{C}_{29}\text{H}_{25}\text{O}_9\text{N}_4$ [M-H] $^-$: $m/z = 573.16270$, found 573.16262.

4.1.7.2.

3-((1-(2-((3,4-dimethoxyphenyl)amino)-2-oxoethyl)-1H-1,2,3-triazol-4-yl)methoxy)-7-methoxy-9-oxo-9H-xanthen-1-yl acetate (**7b**); White solid; Yield 59.2 %; Mp 240-242 °C; Purity 98.4 %; IR(KBr): 3483, 3359, 3144, 3081, 2948, 2833, 1755, 1693, 1658, 1624, 1552, 1521, 1491, 1437, 1364, 1312, 1286, 1241, 1216, 1162, 1065, 1028, 963, 895, 861, 821, 788, 762, 736, 653, 551 cm^{-1} ; ^1H NMR (400 MHz, $\text{DMSO-}d_6$) δ 10.37 (s, 1H), 8.35 (s, 1H), 7.56 (d, $J = 9.0$ Hz, 1H), 7.47 (d, $J = 3.1$ Hz, 1H), 7.41 (dd, $J = 9.0, 3.1$ Hz, 1H), 7.31 (d, $J = 2.3$ Hz, 1H), 7.28 (d, $J = 2.4$ Hz, 1H), 7.06 (dd, $J = 8.6, 2.3$ Hz, 1H), 6.90 (d, $J = 8.6$ Hz, 1H), 6.85 (d, $J = 2.4$ Hz, 1H), 5.40 (s, 2H), 5.35 (s, 2H), 3.86 (s, 3H), 3.71 (s, 6H), 2.37 (s, 3H); ^{13}C NMR (100 MHz, $\text{DMSO-}d_6$) δ 173.47, 168.89, 163.64, 162.82, 158.13, 155.85, 150.96, 149.39, 148.57, 145.15, 141.36, 131.92, 126.89, 124.15, 121.87, 119.18, 112.04, 111.10, 108.17, 107.90, 105.71, 104.26, 99.75, 62.04, 55.70, 55.66, 55.31, 52.23, 21.00; HRMS (ESI) calcd for $\text{C}_{29}\text{H}_{25}\text{O}_9\text{N}_4$ [M-H] $^-$: $m/z = 573.16270$, found 573.16253.

4.1.7.3.

6-bromo-3-((1-(2-((3,4-dimethoxyphenyl)amino)-2-oxoethyl)-1H-1,2,3-triazol-4-yl)methoxy)-9-oxo-9H-xanthen-1-yl acetate (**7c**); White solid ; Yield 80.6 %; Mp 168-170 °C; Purity 97.9 %; IR(KBr): 3514, 3269, 3144, 3084, 2925, 2849, 1767, 1666, 1626, 1598, 1557, 1516, 1418, 1368, 1287, 1221, 1152, 1059, 1024, 973, 919, 895, 845, 726, 663, 551 cm^{-1} ; ^1H NMR (500 MHz, $\text{DMSO-}d_6$) δ 10.39 (s, 1H), 8.35 (s, 1H), 8.00 (d, $J = 8.5$ Hz, 1H), 7.92 (d, $J = 1.8$ Hz, 1H), 7.62 (dd, $J = 8.5, 1.8$ Hz, 1H), 7.30 (d, $J = 2.4$ Hz, 1H), 7.29 (d, $J = 2.4$ Hz, 1H), 7.05 (dd, $J = 8.7, 2.4$ Hz, 1H), 6.93-6.86

(m, 2H), 5.41 (s, 2H), 5.34 (s, 2H), 3.71 (d, $J = 3.1$ Hz, 6H), 2.36 (s, 3H); ^{13}C NMR (125 MHz, DMSO- d_6) δ 173.61, 169.33, 164.10, 163.70, 158.51, 155.47, 151.48, 148.98, 145.57, 141.73, 132.35, 128.73, 128.33, 128.13, 127.40, 121.12, 120.93, 112.44, 111.51, 109.11, 108.77, 104.62, 100.50, 62.59, 56.08, 55.74, 52.67, 21.44; HRMS (ESI) calcd for $\text{C}_{28}\text{H}_{22}\text{O}_8\text{N}_4\text{Br}$ [M-H] $^-$: $m/z = 621.06265$, found 621.06238.

4.1.7.4.

7-bromo-3-((1-(2-((3,4-dimethoxyphenyl)amino)-2-oxoethyl)-1H-1,2,3-triazol-4-yl)methoxy)-9-oxo-9H-xanthen-1-yl acetate (**7d**); White solid; Yield 92.7 %; Mp 204-205 °C; Purity 98.6 %; IR(KBr): 3512, 3259, 3152, 3080, 2939, 2836, 1754, 1664, 1625, 1602, 1556, 1516, 1442, 1369, 1283, 1225, 1151, 1061, 1023, 970, 897, 863, 816, 722, 556 cm^{-1} ; ^1H NMR (400 MHz, DMSO- d_6) δ 10.37 (s, 1H), 8.35 (s, 1H), 8.14 (s, 1H), 7.96 (d, $J = 8.9$ Hz, 1H), 7.58 (d, $J = 8.9$ Hz, 1H), 7.36-7.25 (m, 2H), 7.05 (d, $J = 8.6$ Hz, 1H), 6.95-6.84 (m, 2H), 5.37 (d, $J = 25.0$ Hz, 4H), 3.71 (s, 6H), 2.36 (s, 3H); ^{13}C NMR (100 MHz, DMSO- d_6) δ 172.55, 168.83, 163.63, 163.30, 158.09, 153.77, 151.05, 148.56, 145.15, 141.27, 137.61, 131.90, 127.84, 126.92, 122.95, 120.33, 116.65, 112.03, 111.10, 108.46, 108.31, 104.24, 100.07, 62.14, 55.66, 55.30, 52.23, 20.96; HRMS (ESI) calcd for $\text{C}_{28}\text{H}_{22}\text{O}_8\text{N}_4\text{Br}$ [M-H] $^-$: $m/z = 621.06265$, found 621.06280.

4.1.7.5.

3-((1-(2-((2,4-dimethoxyphenyl)amino)-2-oxoethyl)-1H-1,2,3-triazol-4-yl)methoxy)-6-methoxy-9-oxo-9H-xanthen-1-yl acetate (**7e**); White solid; Yield 89.3 %; Mp 201-203 °C; Purity 99.5 %; IR(KBr): 3413, 3280, 3073, 3008, 2948, 2836, 1756, 1660, 1614, 1542, 1503, 1437, 1363, 1287, 1265, 1209, 1170, 1149, 1067, 1028, 960, 908, 834, 666, 574, 444 cm^{-1} ; ^1H NMR (400 MHz, DMSO- d_6) δ 9.64 (s, 1H), 8.33 (s, 1H), 8.01 (d, $J = 8.9$ Hz, 1H), 7.71 (d, $J = 8.8$ Hz, 1H), 7.24 (d, $J = 2.6$ Hz, 1H), 7.10 (d, $J = 2.4$ Hz, 1H), 7.03 (dd, $J = 8.9, 2.4$ Hz, 1H), 6.86 (d, $J = 2.6$ Hz, 1H), 6.65 (d, $J = 2.7$ Hz, 1H), 6.49 (dd, $J = 8.8, 2.7$ Hz, 1H), 5.41 (d, $J = 12.2$ Hz, 4H), 3.92 (s, 3H), 3.85 (s, 3H), 3.75 (s, 3H), 2.36 (s, 3H); ^{13}C NMR (100 MHz, DMSO- d_6) δ 172.91, 168.89,

164.61, 164.04, 162.60, 158.14, 157.05, 156.64, 151.33, 151.01, 141.37, 127.39, 126.84, 123.35, 119.55, 115.21, 113.51, 108.55, 107.73, 104.11, 100.23, 99.95, 98.89, 62.02, 56.12, 55.76, 55.30, 52.13, 21.02; HRMS (ESI) calcd for C₂₉H₂₅O₉N₄ [M-H]⁻: m/z = 573.16270, found 573.16277.

4.1.7.6.

3-((1-(2-((2,4-dimethoxyphenyl)amino)-2-oxoethyl)-1H-1,2,3-triazol-4-yl)methoxy)-7-methoxy-9-oxo-9H-xanthen-1-yl acetate (**7f**); White solid; Yield 87.1 %; Mp 247-248 °C; Purity 98.2 %; IR(KBr): 3401, 3162, 3076, 3008, 2976, 2939, 2839, 1758, 1692, 1629, 1532, 1490, 1439, 1365, 1287, 1217, 1141, 1061, 1031, 979, 957, 898, 848, 806, 735, 703, 679, 600, 550, 514 cm⁻¹; ¹H NMR (400 MHz, DMSO-*d*₆) δ 9.64 (s, 1H), 8.33 (s, 1H), 7.71 (d, *J* = 8.8 Hz, 1H), 7.57 (d, *J* = 9.0 Hz, 1H), 7.48 (d, *J* = 3.1 Hz, 1H), 7.42 (dd, *J* = 9.0, 3.1 Hz, 1H), 7.28 (d, *J* = 2.4 Hz, 1H), 6.85 (d, *J* = 2.4 Hz, 1H), 6.64 (d, *J* = 2.7 Hz, 1H), 6.48 (dd, *J* = 8.8, 2.7 Hz, 1H), 5.40 (d, *J* = 12.6 Hz, 4H), 3.85 (d, *J* = 6.7 Hz, 6H), 3.74 (s, 3H), 2.37 (s, 3H); ¹³C NMR (100 MHz, DMSO-*d*₆) δ 173.43, 168.80, 163.97, 162.79, 158.09, 157.02, 155.83, 151.31, 150.93, 149.37, 141.31, 126.74, 124.08, 123.31, 121.85, 119.54, 119.13, 108.15, 107.85, 105.75, 104.12, 99.74, 98.89, 62.03, 55.73, 55.68, 55.26, 52.10, 20.94; HRMS (ESI) calcd for C₂₉H₂₅O₉N₄ [M-H]⁻: m/z = 573.16270, found 573.16274.

4.1.7.7.

6-bromo-3-((1-(2-((2,4-dimethoxyphenyl)amino)-2-oxoethyl)-1H-1,2,3-triazol-4-yl)methoxy)-9-oxo-9H-xanthen-1-yl acetate (**7g**); White solid; Yield 87.3 %; Mp 236-240 °C; Purity 95.7 %; IR(KBr): 3293, 3146, 3086, 2938, 2836, 1765, 1667, 1626, 1599, 1554, 1505, 1443, 1418, 1366, 1282, 1214, 1153, 1062, 1026, 961, 914, 829, 727, 662, 632, 565, 514 cm⁻¹; ¹H NMR (500 MHz, DMSO-*d*₆) δ 9.65 (s, 1H), 8.32 (s, 1H), 7.99 (d, *J* = 8.4 Hz, 1H), 7.92 (d, *J* = 1.8 Hz, 1H), 7.70 (d, *J* = 8.9 Hz, 1H), 7.62 (dd, *J* = 8.4, 1.8 Hz, 1H), 7.28 (d, *J* = 2.6 Hz, 1H), 6.90 (d, *J* = 2.6 Hz, 1H), 6.64 (d, *J* = 2.7 Hz, 1H), 6.48 (dd, *J* = 8.9, 2.7 Hz, 1H), 5.41 (d, *J* = 8.1 Hz, 4H), 3.84 (s, 3H), 3.74 (s, 3H), 2.36 (s, 3H); ¹³C NMR (125 MHz, DMSO-*d*₆) δ 173.20, 168.91, 164.08,

163.28, 158.08, 157.06, 155.05, 151.35, 151.06, 141.28, 128.30, 127.91, 127.72, 126.96, 123.39, 120.70, 120.52, 119.55, 108.70, 108.35, 104.09, 100.08, 98.90, 62.16, 55.79, 55.33, 52.14, 21.02; HRMS (ESI) calcd for $C_{28}H_{22}O_8N_4Br$ $[M-H]^-$: $m/z = 621.06265$, found 621.06258.

4.1.7.8.

7-bromo-3-((1-(2-((2,4-dimethoxyphenyl)amino)-2-oxoethyl)-1H-1,2,3-triazol-4-yl)methoxy)-9-oxo-9H-xanthen-1-yl acetate (**7h**); White solid; Yield 87.7 %; Mp 164-166 °C; Purity 99.5 %; IR(KBr): 3475, 3281, 3130, 3065, 2949, 2836, 1773, 1659, 1626, 1602, 1541, 1508, 1436, 1439, 1368, 1309, 1280, 1206, 1147, 1062, 1034, 966, 928, 893, 818, 723, 694, 673, 580, 525 cm^{-1} ; 1H NMR (400 MHz, DMSO- d_6) δ 9.63 (s, 1H), 8.32 (s, 1H), 8.15 (d, $J = 2.6$ Hz, 1H), 7.98 (dd, $J = 8.9, 2.6$ Hz, 1H), 7.70 (d, $J = 8.8$ Hz, 1H), 7.61 (d, $J = 8.9$ Hz, 1H), 7.32 (d, $J = 2.4$ Hz, 1H), 6.90 (d, $J = 2.4$ Hz, 1H), 6.64 (d, $J = 2.7$ Hz, 1H), 6.48 (dd, $J = 8.8, 2.7$ Hz, 1H), 5.41 (d, $J = 4.4$ Hz, 4H), 3.84 (s, 3H), 3.74 (s, 3H), 2.36 (s, 3H); ^{13}C NMR (100 MHz, DMSO- d_6) δ 172.56, 168.84, 164.04, 163.32, 158.09, 157.04, 153.78, 151.32, 151.05, 141.25, 137.63, 127.84, 126.91, 123.35, 122.96, 120.35, 119.55, 116.65, 108.46, 108.32, 104.09, 100.07, 98.88, 62.16, 55.76, 55.30, 52.13, 20.96; HRMS (ESI) calcd for $C_{28}H_{22}O_8N_4Br$ $[M-H]^-$: $m/z = 621.06265$, found 621.06289.

4.2 Biological study

4.2.1 α -glucosidase inhibitory assays

The method for determining the inhibitory activities in this study was similar to those reported previously [17, 37, 38]. Briefly, α -glucosidase activity was assayed in phosphate buffer (50 mM, pH 6.8) containing 5% v/v DMSO using p-nitrophenyl- α -D-glucopyranoside (PNP) as a substrate. The inhibitors and enzyme were pre-incubated in phosphate buffer for 30 min at 37 °C. PNP glucoside was added, and then the enzymatic reaction was carried out for 1 min at 37 °C. The reaction was monitored spectrophotometrically by measuring the absorbance at 400 nm. The IC_{50} values were estimated with five different inhibitory concentrations around IC_{50} values

after preliminary estimation of the first round of experiment. Each sample was measured three times in parallel.

4.2.2 Kinetics of α -glucosidase inhibitors

The kinetics of enzyme inhibition were determined from Lineweaver Burk plots, using the methods similar to those reported in literature [37, 38]. Different concentrations of both inhibitors around the IC_{50} values and the substrate were chosen. With each concentration of inhibitors, α -glucosidase activity was assayed by varying the concentration of PNP glycoside. The enzyme inhibition was performed with the same assays detailed above. The inhibitors and enzyme were pre-incubated in phosphate buffer at 37 °C for 30 min. the substrate was added, and then the enzymatic reaction was carried out at 37 °C for 1 min. The reaction was monitored spectrophotometrically by measuring the absorbance at 400 nm. Inhibition types of the inhibitors were obtained using double-reciprocal plots.

4.2.3 Cell cultures

The human hepatoma cell line (HepG2) and human hepatocyte cell line (LO2) were Cells were cultured in DMEM (Gibco, USA) containing 10 % fetal bovine serum (Gibco, USA), 100 units/mL penicillin and 100 μ g/mL streptomycin (BI, USA), in a humid atmosphere at 37 °C with 5 % CO_2 .

4.2.4 Cell viability assay.

An MTT assay was used to measure the proliferation of cells treated with different compounds in 96-well plates [40]. Briefly, cells were plated in 96-well culture plates at the density of 5000 cells per well in DMEM medium with 200 μ L aliquots and left at 37 °C in 5 % atmosphere. After 24 h incubation, the cells were treated with test compounds at various concentrations for 44 h. 20 μ L (5 mg/mL) MTT was added to each well thereafter and incubated for another 4 h. The supernatant was discarded, and 150 μ L DMSO was added into each well and then the absorbance (A) was measured at 490 nm using a microplate reader (Bio-Rad, USA). Cell viability was

calculated using the following equation, Cell viability (%) = $(A_{\text{treated}}) / (A_{\text{control}}) \times 100$ %. IC₅₀ value was the concentration that caused 50% inhibition of cell viabilities [41].

4.2.5 Total glucose uptake assay

The effect of xanthone-triazole derivatives on total glucose uptake in HepG2 were assessed as described previously with slight modifications [38, 42]. HepG2 cells were cultured in high-glucose DMEM supplemented with 10 % fetal bovine serum, 100 units/mL penicillin and 100 µg/mL streptomycin, in a humid atmosphere of 95 % air-5 % CO₂ at 37°C. After achieving confluence, the cells were seeded in 96-well cluster plates at the density of 5000 cells and cultured in the same medium for 24 h. Following this incubation, the cells were washed three times with low-glucose DMEM and twice phosphate-buffered saline. The cells were added in low-glucose DMEM with 2 % fetal bovine serum containing the various test compounds at different concentrations. After 24 h glucose uptake by HepG2 cells, the remaining glucose in the medium was measured by Glucose Analysis Kit (Jian Cheng, China).

4.3 Molecular Docking Studies

The homology model of α-glucosidase, using oligo-1,6-glucosidase from *Saccharomyces cerevisiae* (PDB: 3AXH) as the template (sequence identity: 72.51 %), was retrieved from SWISS-MODEL Repository for docking studies. Gasteiger partial charges were assigned and non-polar hydrogen atoms were merged with AutoDock Tools [43, 44]. The ligands were structured and optimized by ChemBioDraw Ultra 12.0, ChemBio3D Ultra 12.0 and Gaussian 09 W, following by format transformation to PDBQT files using Autodock Tools. Autodock 4.2.6[44-46] was assigned to perform the docking studies and the Autodock Tools was generated to visualize the results of the docking procedures.

Acknowledgements

We thank Dr. Yong Rao (*Sun Yat-sen University*) for guiding our glucose uptake assay

and Prof. Wei Xia (*Sun Yat-sen University*) for providing us with equipment for cell culture.

This research was supported by the National Natural Science Foundation of China (21272290, J1103305) and the Fund for Innovative Chemical Experiment and Research of School of Chemistry and Sun Yat-sen University.

References

- [1] C. Philip, M. Goedert. GSK3 inhibitors: Development and therapeutic potential. *Nat. Rev. Drug. Discov.*, 3 (2004), 479-487.
- [2] B Michael. Biochemistry and molecular cell biology of diabetic complications. *Nature.*, 414 (2001), 813-820.
- [3] S.P. Marso, W.R. Hiatt, Peripheral arterial disease in patients with diabetes, *J. Am. Coll. Cardiol.*, 47 (2006), 921-929.
- [4] S.P. Kasturi, S. Surarapu, S. Uppalanchi, S. Dwivedi, P. Yogeewari, D.K. Sigalapalli, N.B. Bathini, K.S. Ethiraj, J.S. Anireddy, Synthesis, molecular modeling and evaluation of α -glucosidase inhibition activity of 3,4-dihydroxy piperidines, *Eur. J. Med. Chem.*, 150 (2018), 39-52.
- [5] <https://www.who.int/news-room/fact-sheets/detail/diabetes>.
- [6] J.E. Reusch, J.E. Manson, Management of type 2 diabetes in 2017: Getting to goal, *Jama.*, 317 (2017), 1015-1016.
- [7] C. Proença, M. Freitas, D. Ribeiro, E.F. Oliveira, J.L. Sousa, S.M. Tomé, M.J. Ramos, A.M. Silva, P.A. Fernandes, E. Fernandes, α -Glucosidase inhibition by flavonoids: An in vitro and in silico structure-activity relationship study, *J. Enzym. Inhib. Med. Ch.*, 32 (2017), 1216-1228.
- [8] J.B. Xiao, P. Hogger, Dietary polyphenols and type 2 diabetes: Current insights and future perspectives, *Curr. Med. Chem.*, 22 (2015), 23-38.
- [9] C.M. Ma, M. Hattori, M. Daneshtalab, L. Wang, Chlorogenic acid derivatives with alkyl chains of different lengths and orientations: Potent α -Glucosidase inhibitors, *J. Med. Chem.*, 51 (2008), 6188-6194.

- [10] L. Zeng, G. Zhang, Y. Liao, D. Gong, Inhibitory mechanism of morin on α -glucosidase and its anti-glycation properties, *Food Funct.*, 7 (2016), 3953-3963.
- [11] T.T. Chai, M.T. Kwek, H.C. Ong, F.C. Wong, Water fraction of edible medicinal fern *Stenochlaena palustris* is a potent α -glucosidase inhibitor with concurrent antioxidant activity, *Food Chem.*, 186 (2015), 26-31.
- [12] B.R.P. Kumar, M. Soni, S.S. Kumar, K. Singh, M. Patil, R.B.N. Baig, L. Adhikary, Synthesis, glucose uptake activity and structure-activity relationships of some novel glitazones incorporated with glycine, aromatic and alicyclic amine moieties via two carbon acyl linker, *Eur. J. Med. Chem.*, 46 (2011), 835-844.
- [13] G.T.T. Ho, T.K.Y. Nguyen, E.T. Kase, M. Tadesse, H. Barsett, H. Wangenstein, Enhanced glucose uptake in human liver cells and inhibition of carbohydrate hydrolyzing enzymes by nordic berry extracts, *Molecules*, 22 (2017), 1806.
- [14] V. Peres, T.J. Nagem, F.F. de Oliveira, Tetraoxygenated naturally occurring xanthenes, *Phytochemistry*, 55 (2000), 683-710.
- [15] J. Pedraza-Chaverri, N. Cárdenas-Rodríguez, M. Orozco-Ibarra, J.M. Pérez-Rojas, Medicinal properties of mangosteen (*Garcinia mangostana*), *Food. Chem. Toxicol.*, 46 (2008), 3227-3239.
- [16] J.S. Negi, V.K. Bisht, P. Singh, M. Rawat, G.P. Joshi, Naturally occurring xanthenes: Chemistry and biology, *J. Appl. Chem.*, 2013 (2013), 1-9.
- [17] Y. Liu, L. Zou, L. Ma, W. Chen, B. Wang, Z. Xu, Synthesis and pharmacological activities of xanthone derivatives as α -glucosidase inhibitors, *Bioorg. Med. Chem.*, 14 (2006), 5683-5690.
- [18] Y. Liu, L. Ma, W. Chen, B. Wang, Z.L. Xu, Synthesis of xanthone derivatives with extended π systems as α -glucosidase inhibitors: Insight into the probable binding mode, *Bioorg. Med. Chem.*, 15 (2007), 2810-2814.
- [19] G.L. Li, J.Y. He, A. Zhang, Y. Wan, B. Wang, W.H. Chen, Toward potent α -glucosidase inhibitors based on xanthenes: A closer look into the structure-activity correlations, *Eur. J. Med. Chem.*, 46 (2011), 4050-4055.

- [20] S.M. Ding, T. Lan, G.J. Ye, J.J. Huang, Y. Hu, Y.R. Zhu, B. Wang, Novel oxazolxanthone derivatives as a new type of α -glucosidase inhibitor: Synthesis, activities, inhibitory modes and synergetic effect, *Bioorg. Med. Chem.*, 26 (2018), 3370-3378.
- [21] G.L. Li, C.Y. Cai, J.Y. He, L. Rao, L. Ma, Y. Liu, B. Wang, Synthesis of 3-acyloxyxanthone derivatives as α -glucosidase inhibitors: A further insight into the 3-substituents' effect, *Bioorg. Med. Chem.*, 24 (2016), 1431-1438.
- [22] G.C. Tron, T. Pirali, R.A. Billington, P.L. Canonico, G. Sorba, A.A. Genazzani, Click chemistry reactions in medicinal chemistry: Applications of the 1,3-dipolar cycloaddition between azides and alkynes, *Med. Res. Rev.*, 28 (2008), 278-308.
- [23] S.B. Ferreira, A.C.R. Sodero, M.F.C. Cardoso, E.S. Lima, C.R. Kaiser, F.P. Silva, V.F. Ferreira, Synthesis, biological activity, and molecular modeling studies of 1H-1,2,3-triazole derivatives of carbohydrates as α -glucosidases inhibitors, *J. Med. Chem.*, 53 (2010), 2364-2375.
- [24] A. Lauria, R. Delisi, F. Mingoia, A. Terenzi, A. Martorana, G. Barone, A.M. Almerico, 1,2,3-Triazole in Heterocyclic Compounds, Endowed with Biological Activity, through 1,3-Dipolar Cycloadditions, *Eur. J. Org. Chem.*, 16 (2014), 3289-3306.
- [25] S.G. Agalave, S.R. Maujan, V.S. Pore, Click Chemistry: 1,2,3-Triazoles as Pharmacophores, *Chem - Asian J*, 6 (2011), 2696-2718.
- [26] G. Wang, Z. Peng, J. Wang, J. Li, X. Li, Synthesis and biological evaluation of novel 2,4,5-triarylimidazole-1,2,3-triazole derivatives via click chemistry as α -glucosidase inhibitors, *Bioorg. Med. Chem. Lett.*, 26 (2016), 5719-5723.
- [27] G. Wang, Z. Peng, J. Wang, X. Li, J. Li, Synthesis, in vitro evaluation and molecular docking studies of novel triazine-triazole derivatives as potential α -glucosidase inhibitors, *Eur. J. Med. Chem.*, 125 (2017), 423-429. [28] G. Ho, E. Kase, H. Wangenstein, H. Barsett, Effect of phenolic compounds from elderflowers on glucose-and fatty acid uptake in human myotubes and HepG2-cells, *Molecules.*, 22 (2017), 90.

- [29] T. Zhou, Q. Shi, C. Chen, L. Huang, P. Ho, S.L. Morris-Natschke, K. Lee, Anti-AIDS agents 85. Design, synthesis, and evaluation of 1R,2R-dicamphanoyl-3,3-dimethyldihydropyrano-[2,3-c] xanthen-7(1H)-one (DCX) derivatives as novel anti-HIV agents, *Eur. J. Med. Chem.*, 47 (2012), 86-96.
- [30] W. Zhang, Z. Li, M. Zhou, F. Wu, X. Hou, H. Luo, H. Liu, X. Han, G. Yan, Z. Ding, Synthesis and biological evaluation of 4-(1, 2, 3-triazol-1-yl) coumarin derivatives as potential antitumor agents, *Bioorg. Med. Chem. Lett.*, 24 (2014), 799-807.
- [31] J.L. Ren, X.Y. Zhang, B. Yu, X.X. Wang, K.P. Shao, X.G. Zhu, H.M. Liu, Discovery of novel AHLs as potent antiproliferative agents, *Eur. J. Med. Chem.*, 93 (2015), 321-329.
- [32] S. Lal, H.S. Rzepa, S. Díez-González, Catalytic and computational studies of N-Heterocyclic carbene or Phosphine-Containing Copper(I) complexes for the synthesis of 5-iodo-1,2,3-triazoles, *ACS Catal.*, 4 (2014), 2274-2287.
- [33] P. Wu, A.K. Feldman, A.K. Nugent, C.J. Hawker, A. Scheel, B. Voit, J. Pyun, J.M.J. Fréchet, K.B. Sharpless, V.V. Fokin, Efficiency and fidelity in a Click-Chemistry route to triazole dendrimers by the Copper(I)-Catalyzed ligation of azides and alkynes, *Angew Chem Int Edit.*, 43 (2004), 3928-3932.
- [34] T.M. Kosak, H.A. Conrad, A.L. Korich, R.L. Lord, Ether cleavage Re-Investigated: Elucidating the mechanism of BBr₃-Facilitated demethylation of aryl methyl ethers, *Eur. J. Org. Chem.*, 34 (2015), 7460-7467.
- [35] C. Prinzisky, I. Meyenburg, A. Jacob, B. Heidelmeier, F. Schröder, W. Heimbrod, J. Sundermeyer, Optical and electrochemical properties of anthraquinone imine based dyes for Dye-Sensitized solar cells, *Eur. J. Org. Chem.*, 4 (2016), 756-767.
- [36] Y. Liu, Z. Ke, J. Cui, W. Chen, L. Ma, B. Wang, Synthesis, inhibitory activities, and QSAR study of xanthone derivatives as α -glucosidase inhibitors, *Bioorg. Med. Chem.*, 16 (2008), 7185-7192.

- [37] Y. Wang, L. Ma, C. Pang, M. Huang, Z. Huang, L. Gu, Synergetic inhibition of genistein and d-glucose on α -glucosidase, *Bioorg. Med. Chem. Lett.*, 14 (2004), 2947-2950.
- [38] H. Sun, X. Song, Y. Tao, M. Li, K. Yang, H. Zheng, Z. Jin, R.H. Dodd, G. Pan, K. Lu, P. Yu, Synthesis & α -glucosidase inhibitory & glucose consumption-promoting activities of flavonoid-coumarin hybrids, *Future Med. Chem.*, 10 (2018), 1055-1066.
- [39] S. Bienert, A. Waterhouse, T.A.P. de Beer, G. Tauriello, G. Studer, L. Bordoli, T. Schwede, The SWISS-MODEL Repository-new features and functionality, *Nucleic Acids Res.*, 45 (2016), D313-D319.
- [40] T. Mosmann, Rapid colorimetric assay for cellular growth and survival: Application to proliferation and cytotoxicity assays, *J. Immunol. Methods.*, 65 (1983), 55-63.
- [41] M. Wang, L. Zhang, X. Han, J. Yang, J. Qian, S. Hong, F. Samaniego, J. Romaguera, Q. Yi, Atiprimod inhibits the growth of mantle cell lymphoma in vitro and in vivo and induces apoptosis via activating the mitochondrial pathways, *Blood.*, (109) 2007, 5455-5462.
- [42] X.C. Tan, K.H. Chua, M.R. Ram, U.R. Kuppusamy, Monoterpenes: Novel insights into their biological effects and roles on glucose uptake and lipid metabolism in 3T3-L1 adipocytes, *Food Chem.*, 196 (2016), 242-250.
- [43] M.F. Sanner, Python: A programming language for software integration and development, *J. Mol. Graph. Model.*, 17 (1999), 57-61.
- [44] G.M. Morris, R. Huey, W. Lindstrom, M.F. Sanner, R.K. Belew, D.S. Goodsell, A.J. Olson, AutoDock4 and AutoDockTools4: Automated docking with selective receptor flexibility, *J. Comput. Chem.*, 30 (2009), 2785-2791.
- [45] S. Cosconati, S. Forli, A.L. Perryman, R. Harris, D.S. Goodsell, A.J. Olson, Virtual screening with AutoDock: Theory and practice, *Expert Opin. Drug Dis.*, 5 (2010), 597-607.
- [46] S. Forli, A.J. Olson, A force field with discrete displaceable waters and

desolvation entropy for hydrated ligand docking, *J. Med. Chem.*, 55 (2012), 623-638.

Tables, figures and scheme

Table 1. *In vitro* α -glucosidase inhibitory activity of compounds **5a-5h**, **6a-6h**, **7a-7h**

Table 2. LO2 cytotoxicity of compounds **5a-5h**, **6a-6h**, **7a-7h**

Figure 1. Xanthenes as α -glucosidase inhibitors and molecular docking of the xanthone-triazole's skeleton. (A) The synthetic xanthenes as the potential α -glucosidase inhibitors. (B) 1,3-dihydroxyxanthone and the skeleton of xanthone-triazole. (C) Predicted interactions of the skeleton of xanthone-triazole with α -glucosidase. The green dashed lines stand for hydrogen bonds.

Figure 2. The structure of flavonoids and xanthone-triazole derivatives.

Figure 3. Lineweaver-Burk plots ($1/V$ vs $1/[S]$) of α -glucosidase inhibition of compounds **5e**, **5g**, **5h**, **6c**, **6d**, **6g** and **6h**.

Figure 4. Binding positions of compounds **5e**, **5g**, **5h**, **6c**, **6d**, **6g** and **6h**. All the examined compounds bind to allosteric sites away from the active site (Asp214, Glu276 and Asp349) of α -glucosidase.

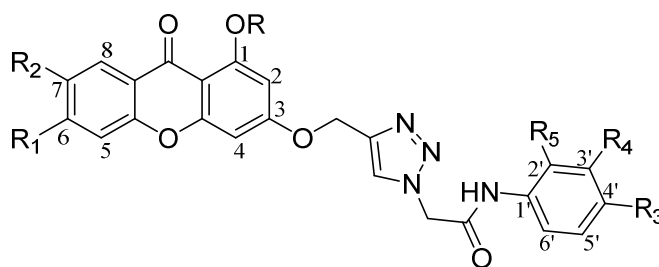
Figure 5. Predicted interactions between α -glucosidase and compounds **6c**, **5e**, **5h** and **6g**. The green dashed lines stand for hydrogen bonds, yellow columns stand for π - π interactions, and yellow cones stand for π -cation interactions. (A) Compound **6c**: Hydrogen bonds, π - π interactions, π -cation interactions. (B) Compound **5e**: Hydrogen bonds, π - π interactions, π -cation interactions. (C) Compound **5h**: Hydrogen bonds, π - π interactions. (D) Compound **6g**: Hydrogen bonds, π - π interactions.

Figure 6. Effects of different concentrations of compounds **a**, **5e**, **5f**, **5g**, **5h**, **6a**, **6b**, **6c**, **6d**, **6g**, **6h**, **7g** and **7h** on HepG2 cells growth.

Figure 7. Effects of compounds **a**, **5e**, **5f**, **5g**, **5h**, **6a**, **6b**, **6c**, **6d**, **6g**, **6h**, **7g** and **7h** on glucose uptake of HepG2 cells.

Scheme 1. Synthesis of xanthone-triazole derivatives. Reagents and conditions: (a) Eaton's reagent, reflux; (b) 3-bromopropyne, K_2CO_3 , acetone, reflux; (c) dry THF, N_2 , 0 °C; (d) NaN_3 , DMF, 40 °C; (e) $CuSO_4 \cdot 5H_2O$, sodium ascorbate, DMF, rt; (f) BBr_3 , dry DCM, 0 °C; (g) Ac_2O , NaOAc, 90 °C.

ACCEPTED MANUSCRIPT

Table 1. *In vitro* α -glucosidase inhibitory activity of compounds **5a-5h**, **6a-6h**, **7a-7h**.

Compounds	R	R ₁	R ₂	R ₃	R ₄	R ₅	IC ₅₀ (μM) ^a
5a	H	OCH ₃	H	OCH ₃	OCH ₃	H	15.90±0.91
5b	H	H	OCH ₃	OCH ₃	OCH ₃	H	>100 ^b
5c	H	Br	H	OCH ₃	OCH ₃	H	11.82±0.82
5d	H	H	Br	OCH ₃	OCH ₃	H	29.84±3.47
5e	H	OCH ₃	H	OCH ₃	H	OCH ₃	2.06±0.16
5f	H	H	OCH ₃	OCH ₃	H	OCH ₃	8.31±0.88
5g	H	Br	H	OCH ₃	H	OCH ₃	2.78±0.22
5h	H	H	Br	OCH ₃	H	OCH ₃	3.07±0.56
6a	H	OH	H	OH	OH	H	6.13±0.09
6b	H	H	OH	OH	OH	H	7.06±0.89
6c	H	Br	H	OH	OH	H	5.23±0.53
6d	H	H	Br	OH	OH	H	3.17±0.61
6e	H	OH	H	OH	H	OH	17.61±1.68
6f	H	H	OH	OH	H	OH	15.62±1.13
6g	H	Br	H	OH	H	OH	5.87±0.76
6h	H	H	Br	OH	H	OH	5.88±0.32
7a	OAc	OCH ₃	H	OCH ₃	OCH ₃	H	98.63±4.12
7b	OAc	H	OCH ₃	OCH ₃	OCH ₃	H	>100 ^b
7c	OAc	Br	H	OCH ₃	OCH ₃	H	26.11±2.95
7d	OAc	H	Br	OCH ₃	OCH ₃	H	32.33±0.82
7e	OAc	OCH ₃	H	OCH ₃	H	OCH ₃	33.16±2.51
7f	OAc	H	OCH ₃	OCH ₃	H	OCH ₃	42.60±0.09
7g	OAc	Br	H	OCH ₃	H	OCH ₃	12.78±0.01
7h	OAc	H	Br	OCH ₃	H	OCH ₃	12.13±1.84

^a IC₅₀ value: concentration that inhibits the activity of α -glucosidase by 50 % (mean \pm SD). The IC₅₀ value of positive control (1-deoxynojirimycin, PG) is 59.50 \pm 4.7 μ M. The IC₅₀ value of parental compound **a** is 160.8 μ M^[17], and compound **b** is 10.6 μ M^[21].

^b Compounds precipitated when the concentration are higher than 100 μ M, but the inhibition is lower than 50 %. Therefore, the IC₅₀ value of compounds **5b** and **7b** can not be obtained.

Table 2. LO2 cytotoxicity of compounds **5a-5h, 6a-6h,7a-7h**

Compounds	IC ₅₀ (μM)	Compounds	IC ₅₀ (μM)	Compounds	IC ₅₀ (μM) ^a
5a	>100	6a	>100	7a	>100
5b	>100	6b	>100	7b	24.92±2.38
5c	>100	6c	>100	7c	25.95±3.10
5d	>100	6d	>100	7d	>100
5e	89.06±4.89	6e	>100	7e	>100
5f	65.43±3.51	6f	>100	7f	>100
5g	>100	6g	73.95±6.73	7g	>100
5h	>100	6h	>100	7h	80.72±1.63

^a IC₅₀ value: concentration that inhibits cells survival by 50 % (means ± SD).

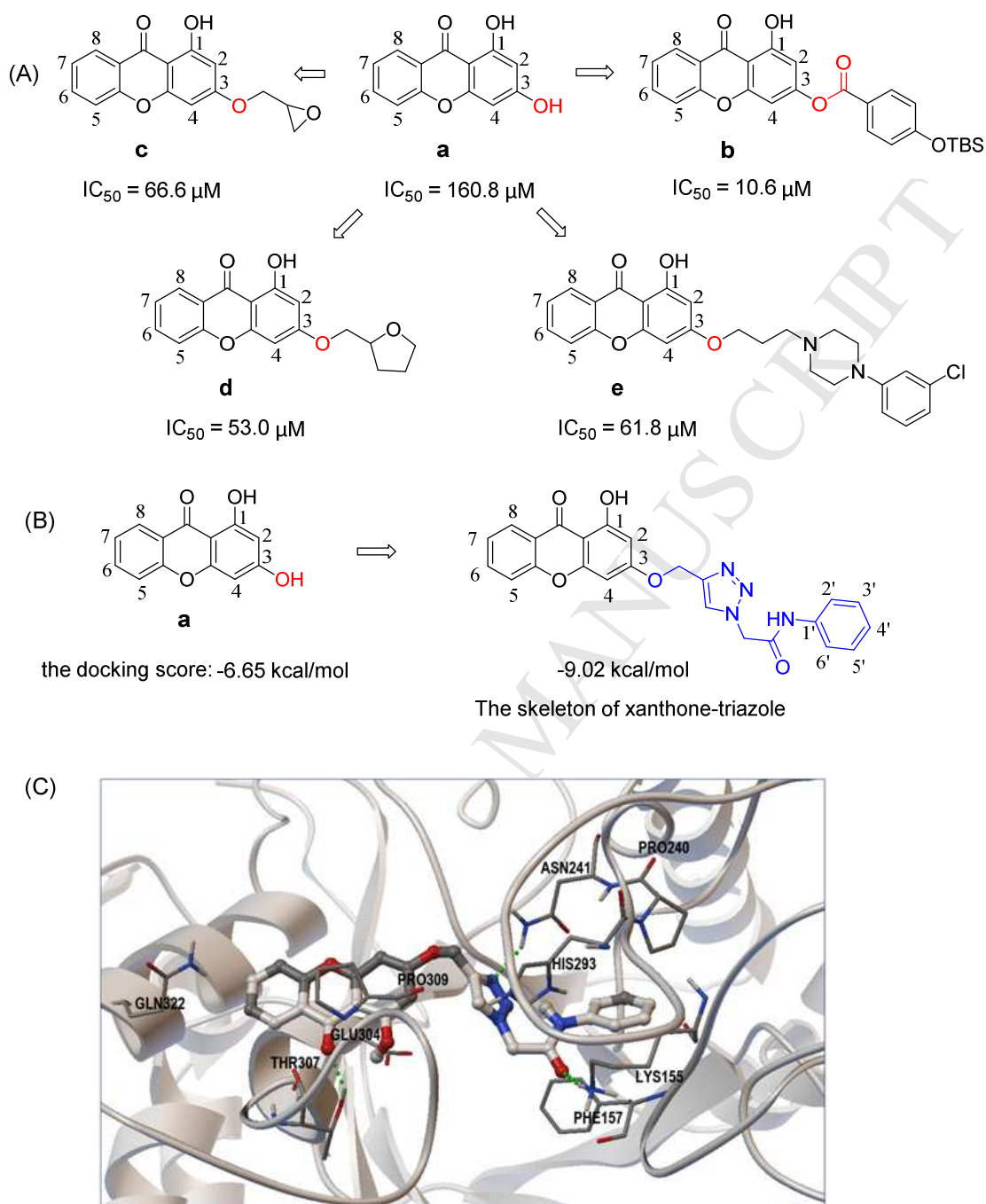
Figure 1.

Figure 1. Xanthenes as α -glucosidase inhibitors and molecular docking of the xanthone-triazole's skeleton. (A) The synthetic xanthenes as the potential α -glucosidase inhibitors. (B) 1,3-dihydroxyxanthone and the skeleton of xanthone-triazole. (C) Predicted interactions of the skeleton of xanthone-triazole with α -glucosidase. The green dashed lines stand for hydrogen bonds.

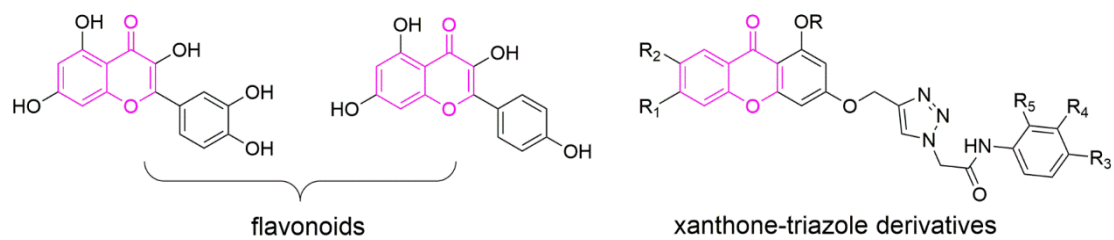
Figure 2.**Figure 2.** The structure of flavonoids and xanthone-triazole derivatives.

Figure 3.

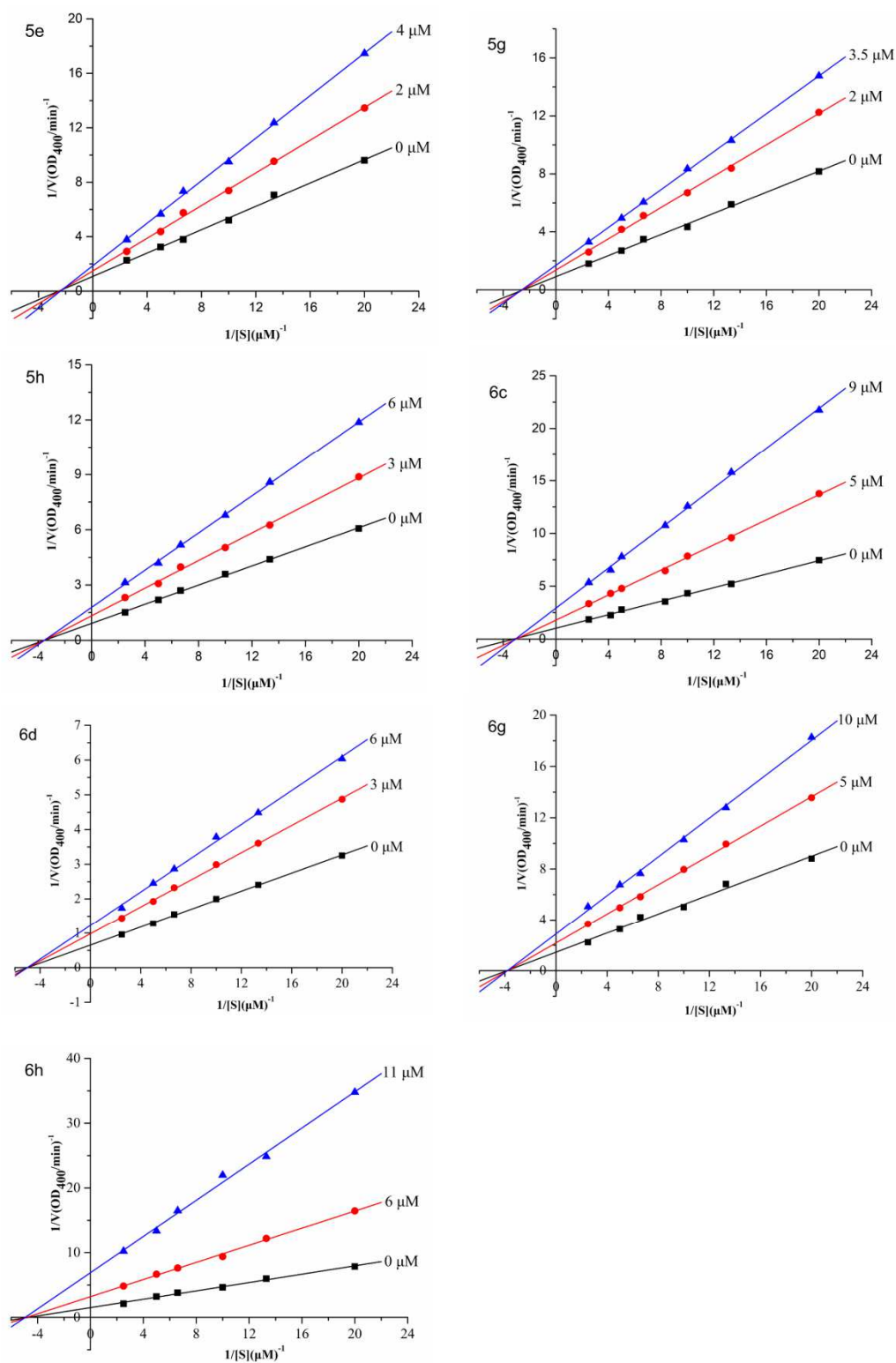


Figure 3. Lineweaver-Burk plots (1/V vs 1/[S]) of α -glucosidase inhibition of compounds 5e, 5g, 5h, 6c, 6d, 6g and 6h.

Figure 4.

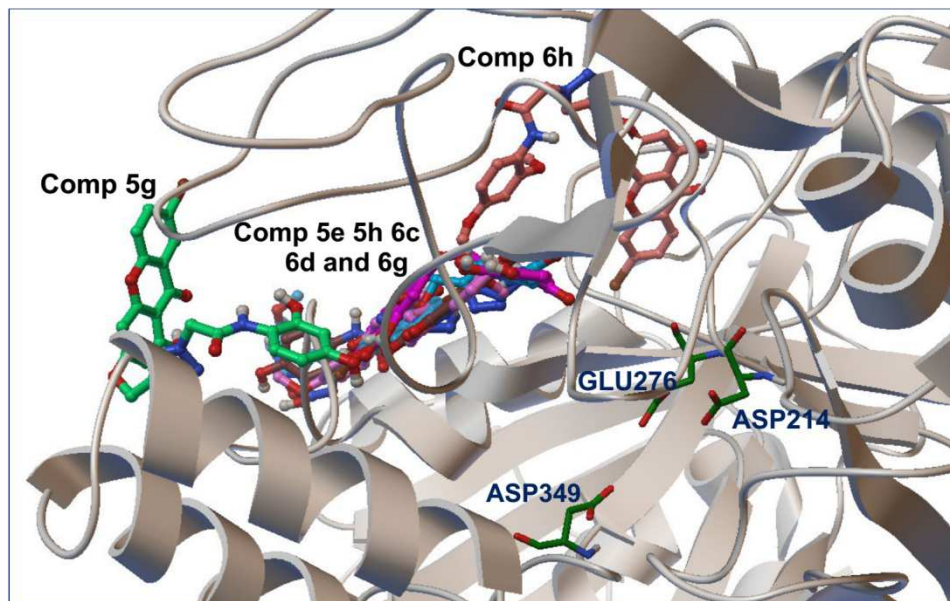


Figure 4. Binding positions of compounds **5e**, **5g**, **5h**, **6c**, **6d**, **6g** and **6h**. All the examined compounds bind to allosteric sites away from the active site (Asp214, Glu276 and Asp349) of α -glucosidase.

Figure 5.

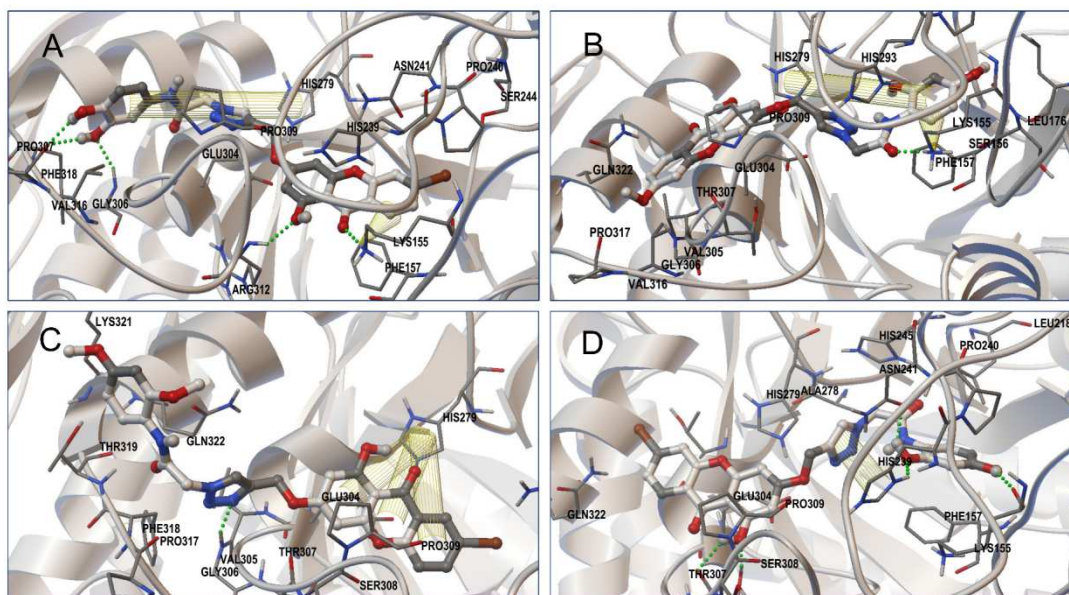


Figure 5. Predicted interactions between α -glucosidase and compounds **6c**, **5e**, **5h** and **6g**. The green dashed lines stand for hydrogen bonds, yellow columns stand for π - π interactions, and yellow cones stand for π -cation interactions. (A) Compound **6c**: Hydrogen bonds, π - π interactions, π -cation interactions. (B) Compound **5e**: Hydrogen

bonds, π - π interactions, π -cation interactions. (C) Compound **5h**: Hydrogen bonds, π - π interactions. (D) Compound **6g**: Hydrogen bonds, π - π interactions.

Figure 6.

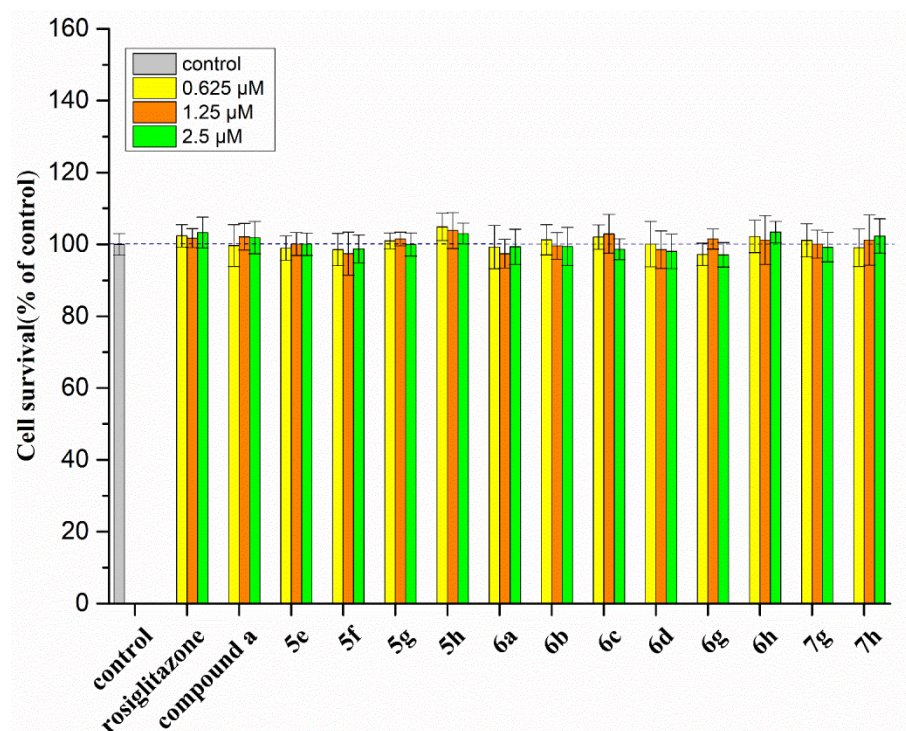
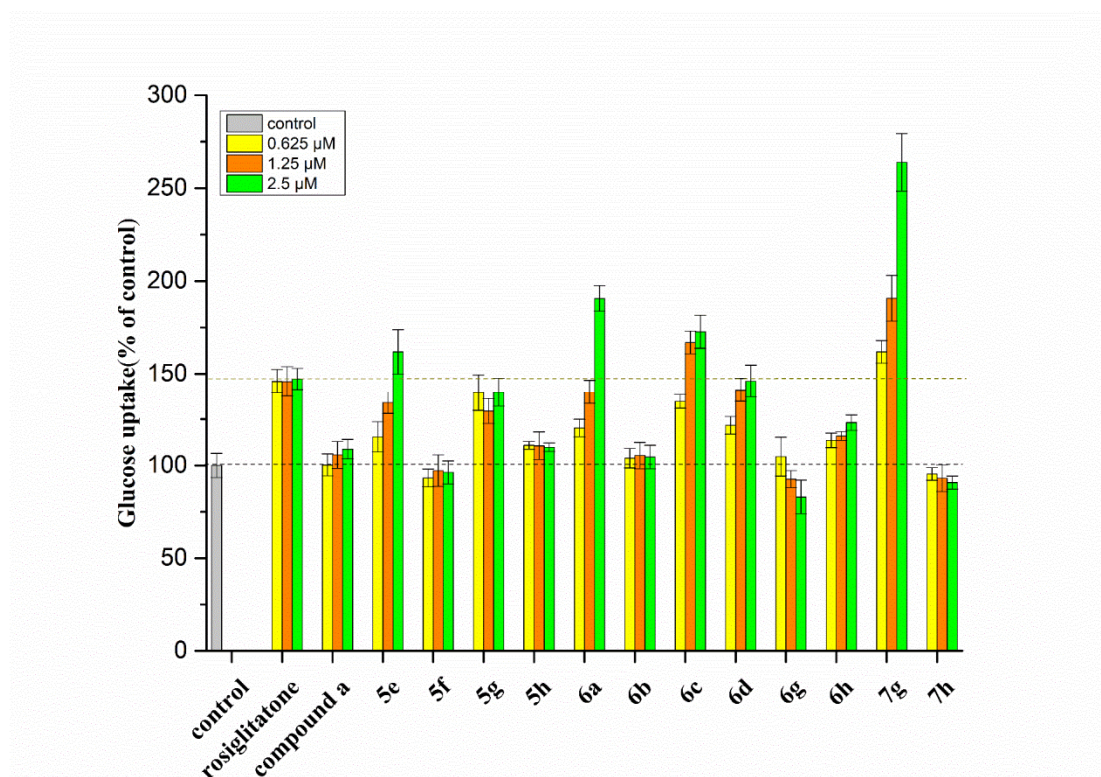
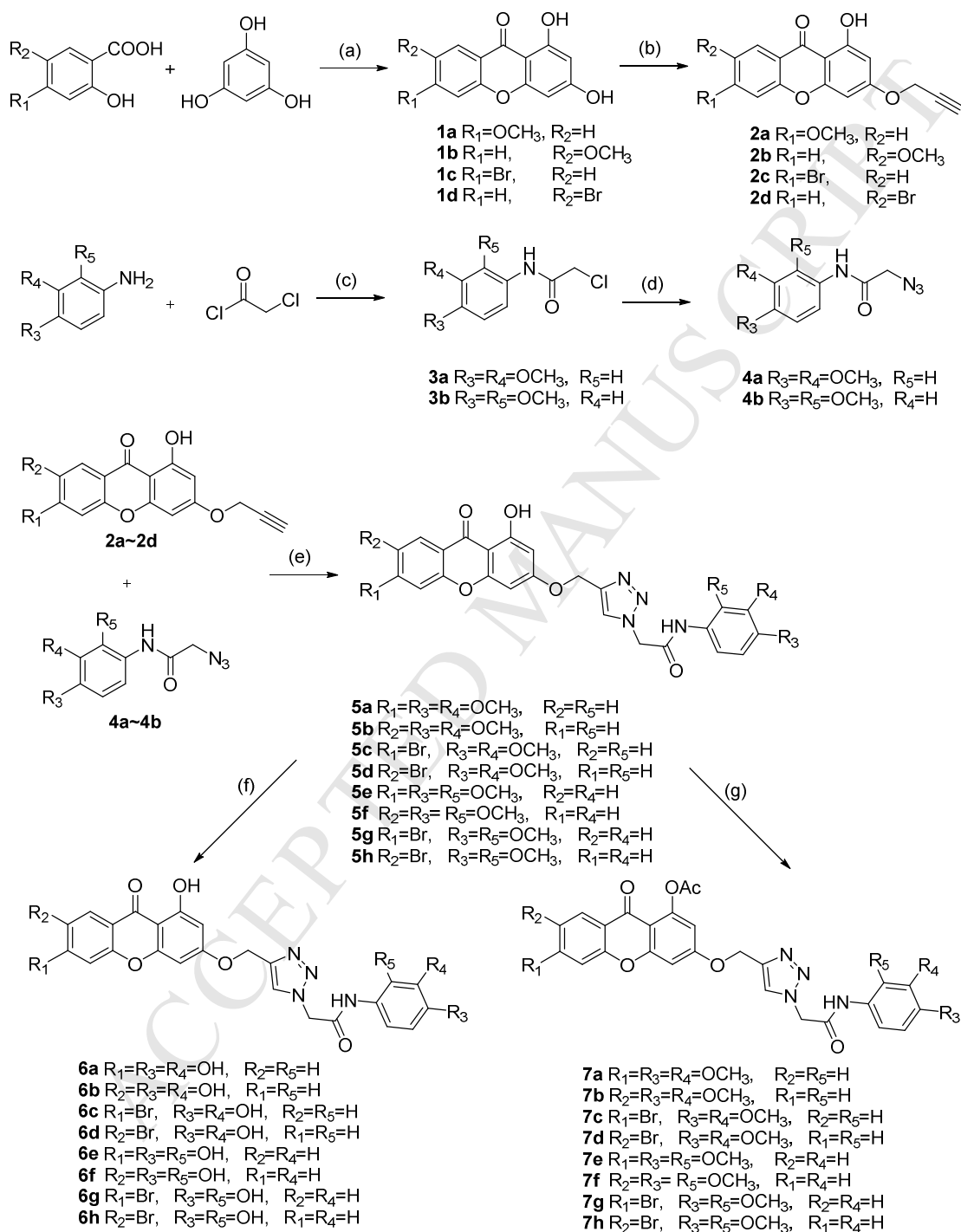


Figure 6. Effects of different concentrations of compounds **a**, **5e**, **5f**, **5g**, **5h**, **6a**, **6b**, **6c**, **6d**, **6g**, **6h**, **7g** and **7h** on HepG2 cells growth.

Figure 7.**Figure 7.** Effects of compounds **a**, **5e**, **5f**, **5g**, **5h**, **6a**, **6b**, **6c**, **6d**, **6g**, **6h**, **7g** and **7h** on glucose uptake of HepG2 cells.

Scheme 1.



Scheme 1. Synthesis of xanthone-triazole derivatives. Reagents and conditions: (a) Eaton's reagent, reflux; (b) 3-bromopropyne, K_2CO_3 , acetone, reflux; (c) dry THF, N_2 , 0 °C; (d) NaN_3 ,

DMF, 40 °C; (e) CuSO₄·5H₂O, sodium ascorbate, DMF, rt; (f) BBr₃, dry DCM, 0 °C; (g) Ac₂O, NaOAc, 90 °C.

ACCEPTED MANUSCRIPT

Highlights

1. Twenty-four novel xanthone-triazole derivatives were designed and synthesized.
2. Xanthone-triazole derivatives significantly increased α -glucosidase inhibition.
3. **5e**, **6a**, **6c** and **7g** had dual effects on α -glycosidase inhibition and glucose uptake.
4. Most of xanthone-triazole derivatives had low toxicity.